THE MEASUREMENT OF XENON-HYDRATES

ABOVE 273.0 $^{\circ}$K

by

Mohamed M. Amer

ProQuest Number: 10782286

ProQuest 10782286

Published by ProQuest LLC (2018). Copyright of the Dissertation is held by the Author.
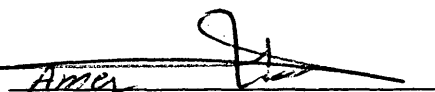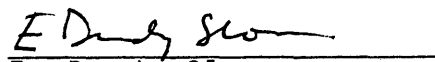
ProQuest LLC.
789 East Eisenhower Parkway
P.O. Box 1346
Ann Arbor, MI 48106 – 1346

A thesis submitted to the Faculty and the Board of
Trustees of the Colorado School of Mines in partial ful-
fillment of the requirements for the degree of Master of
Science (Chemical and Petroleum-Refining Engineering).

Golden, Colorado

Date _December 2, 1981_

Signed: _____
Mohamed Amer

Approved: _____
E. Dendy Sloan
Thesis Advisor

Golden, Colorado

Date _December 2, 1981_

_____
Philip F. Dickson-Professor
and Head, Chemical and
Petroleum-Refining
Engineering

DEDICATION

I Wish to Dedicate this Thesis to my Parents

ABSTRACT

The natural gas hydrates are becoming a major energy resource. Production of these resources depend on the dissociation conditio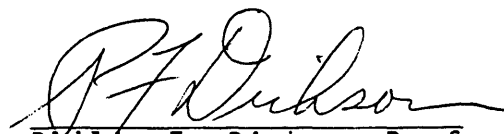ns. The model which predicts dissociation uses xenon hydrate as a reference below 0^oC. There are some large discrepancies in the xenon hydrate data currently in the literature.

This work experimentally determined the dissociation pressure of xenon-water hydrate at temperatures above 0^oC. Data by S. L. Miller was available below 0^oC. The Van der Waals-Platteeuw theory and Parrish-Prausnitz model were used to calculate xenon-water dissociation pressure. Experimental and calculated results were in a good agreement. Kihara parameters and cage occupancy ratios were obtained.

TABLE OF CONTENTS

TABLE OF CONTENTS (CONT.)

LIST OF FIGURES

LIST OF TABLES

ACKNOWLEDGEMENTS

INTRODUCTION

Natural gases under pressure unite with water to form crystalline hydrates at temperatures both below and considerably above $32°F$. The accumulation of liquid water in a natural gas pipe line with favorable conditions of pressure and temperature may cause the line to become plugged with a solid phase.

Early work on hydrates of gaseous substances carried on during the period of theortical studies by Villard (1, 2, 3), de Forcrand (4), and others was reviewed by Schroeder. Hammerschmidt (5, 6, 7) discovered that gas hydrates were the cause of plugged natural gas pipelines. Since then, hydrate formation has become of interest in chemical technology, especially in the natural gas industry. However, any situation in which water and light hydrocarbon gases come into contact at low temperatures, high pressure can cause hydrates to form. Additionally, hydrates have been suggested for use in underground storage of gases (9), for desalinization of sea water (9, 10), and for gas separation (11). Because a knowledge of hydrate forming temperatures and pressures are needed in these instances, the conditions for hydrate formation have been studied extensively.

Interest in gas hydrates has been stimulated in recent years by the discovery of oil and natural gas in colder

climatic regions, such as Alaska, Canada's Northwest
Territory, and Russian Siberia. Naturally occurring gas
hydrates have been found in several natural gas reservoirs
and recent studies by Katz et al. (12, 13) have indicated
that hydrates may have formed in some of the oil reservoirs
in these regions. This last prediction was based primarily
upon the discovery of an oil field in Alaska which contained
virtually no n-butane or lighter constituents - precisely the
constituents which can form gas hydrates when contacted with
water. It has been theorized that the methane, ethane, pro-
pane, butane and other light gases could have been removed
sometime in our recent geological past by combining with
water to form hydrates.

If hydrates do exist in petroleum reservoirs, they can
present several obstacles to the production of the reservoir
oil. First, the hydrates increase the viscosity of the oil
by removing the lighter components from it, secondly, the
vapor pressure, or the driving force for the production of
the oil is lowered by hydrate formation since hydrates
remove the gases with the highest vapor pressure. Thirdly,
the hydrates will block the reservoir pores and greatly
reduce the space available for the oil, a problem which
could also occur in natural gas reservoirs. These problems
have resulted in a renewed interest in the conditions at
which hydrates form, especially when the hydrates are formed

from a mixture of hydrate forming constituents, such as
is the case in naturally occurring gas hydrates.

The conditions which promote hydrate formation are:
(1) The gas must be at or below its water dew point with
"free" water present, (2) low temperature, (3) high pres-
sure, (4) high velocities, (5) pressure pulsations, (6)
any type of agitation, (7) introduction of small crystals
of hydrate. The methods now used to control or remove
hydrates are: (1) pressure manipulation, (2) temperature
manipulations, (3) inhibitors, and (4) gas dehydration.

In order to solve the practical problems caused by gas
hydrates, an interesting theoretical model describing their
formation has been developed (15). The nature of gas hydra-
tes is quite unusual in that the water, or host molecules,
form a cage-like structure which entraps the gas or guest
molecule in a non-stoichiometric manner. Only the inter-
action of the guest and host molecules can stabilize the
lattice structure. Another interesting characteristic of
gas hydrates is that two hydrate structures, designated
Structure I and Structure II are known to form from mix-
tures of natural gases and water.

The main objective of this work is to determine the
dissociation pressure of xenon-water experimentally. Xenon
gas was chosen for this experiment because it was used as
reference hydrate for the prediction of natural gas hydrates

below 0 ^{o}C. The data which are available for xenon hydrate
above 0 ^{o}C do not agree with each other as shown in Figure 1.
The dissociation pressure may provide a new potential func-
tion between guest molecules and the cage, as suggested by
Tse and Davidson (14). This work uses a modification of the
statistical thermodynamic equation presented by Parrish and
Prausnitz (15) to predict the dissociation pressure, at a
given temperature.

Xenon-water hydrate, like methane hydrate forms
Structure I. This is, in some sense, a model hydrate because
of the low pressure at which it forms and because, with a
monatomic guest, one doesn't have to worry about a rota-
tional contribution to the partition function. It will be
noticed that although there is a considerable range in
$\Delta \mu_{0,0}$, all of these give very nearly the same degree of
occupancy of the large and small cages as given in Table 1
(14).
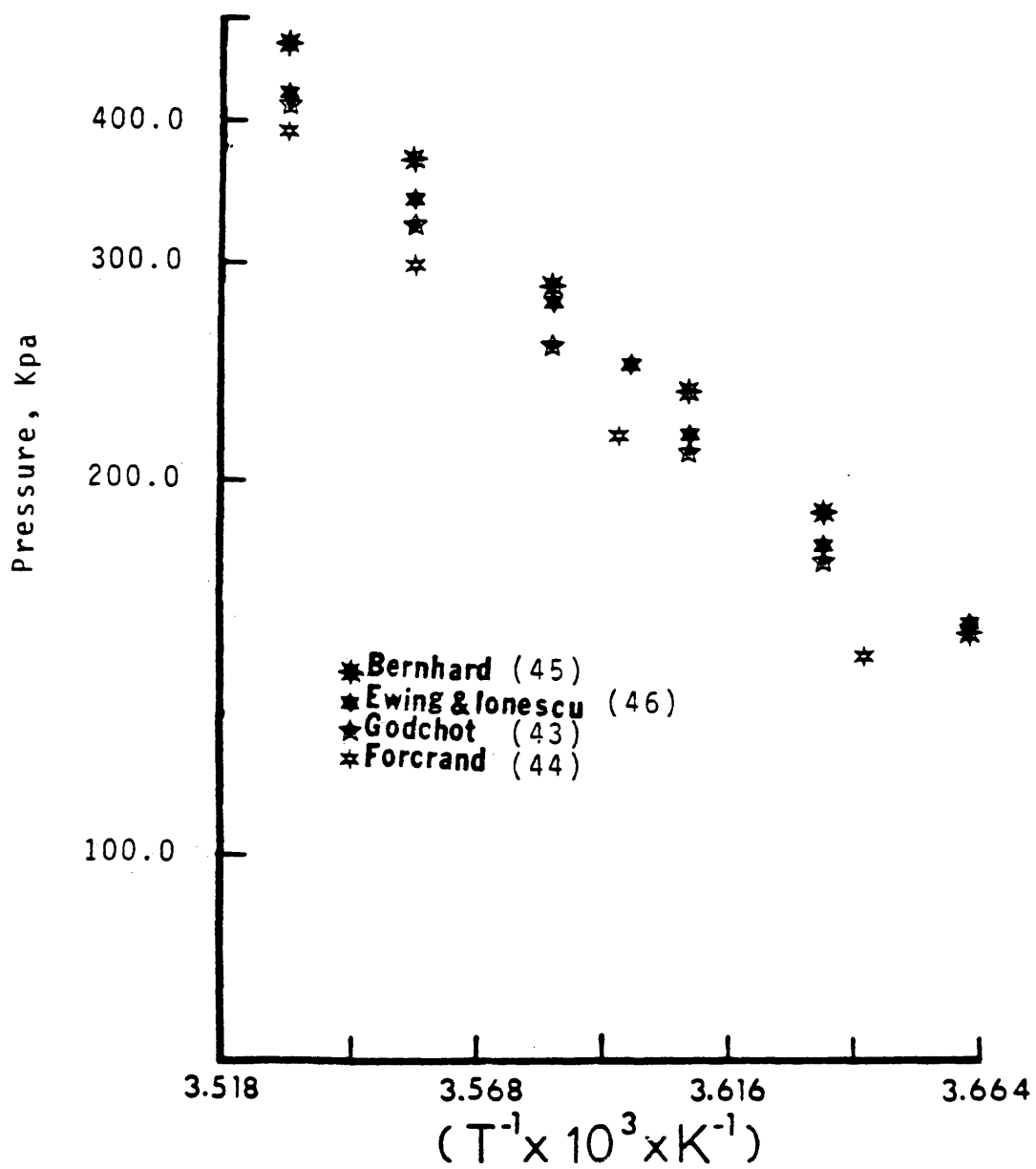
FIGURE 1.

XENON HYDRATE DATA ABOVE 273°K

TABLE 1

CALCULATED OCCUPANCY RATIOS OF CAGES

IN XENON HYDRATE AT 273 °K

Authors	Method	$\Delta\mu$(cal/ mole H_2O)	n	θ_L/θ_S
van der Waals & Platteeuw (34)	Lennard-Jones Devonsshire cell;12-6 potential	167	6.93	1.027
Davidson (14)	Same as above	265	6.12	0.978
Parrish & Prausnitz (15)	L-J-D cell; 12-6 potential with spherical core	302	6.08	1.038
Tester, Bivins & Herrick (14)	Monte Carlo treatment of 12-6 pairwise interactions	302	6.01	0.988
Ripmeester & Davidson (14)	Experiment: $^{129}X_e$ NMR			1.30 ± 0.03

where

$\Delta\mu$ is the assumed excess free energy of water in the empty

hydrate over its value in ice; n is the calculated number

of water molecules per xenon atom in the equilibrium hydrate.

LITERATURE REVIEW

1) History of Gas Hydrates

Gas hydrates are solid crystalline substances with the appearance of snow or loose ice and the general formula M.n H_2O, where M is the hydrate forming molecule. Hydrates are comprised of guest molecules and host molecules. The host molecules (water) form a lattice which is stabilized by the inclusion of the gas molecules.

Clathrate hydrates of gases were first reported in the literature in 1810 by Faraday (16) who attributed their discovery to Sir Humphrey Davy. In the late nineteenth century, Villard, de Forcrand and other investigators found hydrates of many light gases including methane, ethane and propane (17). However, it was not until 1931 that Hammer-schmidt (18) discovered that gas hydrates were the cause of the plugged gas pipelines that were plaguing the natural gas industry. Confirmation by Deaton and Forst (1946) has led to the regulation of the water content of natural gas to the development of improved mehtods of prevention of hydrate plugs (19, 20).

Primarily because of this problem, many studies on the pressures and temperatures of hydrate formation from gases have been done in the last fifty years. These studies were generally aimed at defining the vapor-water-hydrate

equilibrium for binary mixtures of a pure gas and water.
Katz (21) and Scauzillo (22) and other authors (23) reported
studies on lowering the hydrate forming temperature (at a
fixed pressure) by the addition of a non-hydrate forming
substance such as sodium chloride or ethanol to the water
phase. This "anti-freeze" effect was also found to be
present when a non-hydrate former was added to the gas phase.
Excellent detailed reviews of this early work are given by
Katz et al. (24), Byk and Fomina (25), and the API (26).

2) Structure of Gas Hydrates

The hydrate lattice structure was determined through
the x-ray diffraction studies of Von Stackleberg (27),
Pauling and Marsch (28), and Claussen (29). Two types of
hydrate structures, designated structure I and II, were
found to form from light non-polar hydrocarbons.

The hydrates of structure I, Fig. 2 are characterized
by the crystal lattice parameter 12 $\overset{O}{A}$. The unit cell is
constructed from 46 water molecules and in it there are eight
cavities available for gas molecules, including two "small"
cavities and six "large." The "small" cavities of structure
I are regular pentagonal dodecahedra with mean free diameter
$\sim$ 5.1 ^{O}A. Each of the six "large" cavities is tetrahedral
with a mean free diameter of about 5.8 ^{O}A, formed by two
opposing hexagons and 12 pentagons situated between them.
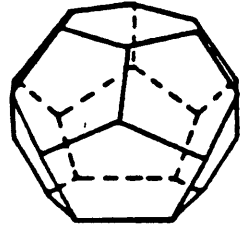
(a) Tetradecahedron (Structure I)
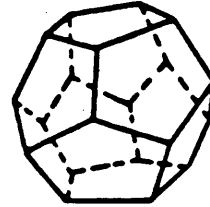
(b) Pentagonal Dodecahedron
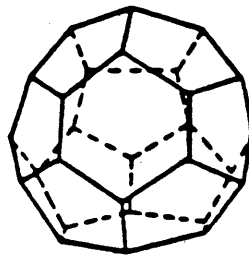
(c) Hexadecahedron (Structure II)
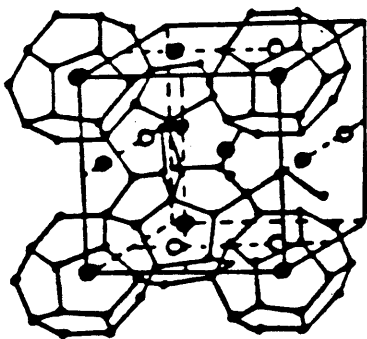
(d)
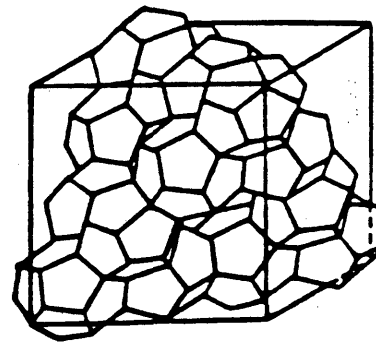
(e)

FIGURE 2.

PACKING OF DODECAHEDRA IN THE HYDRATE UNIT CELL
OF STRUCTURE I (d), AND STRUCTURE II (e). (TAKEN
FROM MENTEN (49)).

The hydrates of structure II, Fig 2 are characterized by the crystal lattice parameter 17.4 ^{O}A. The unit cell is constructed from 136 water molecules, contains 24 cavities, including 16 "small" and 8 "large." The "small" cavities, like in structure I, are pentagonal dodecahedra, but somewhat deformed as a result of which the mean free diameter is $\sim$ 5 ^{O}A. The "large" cavities of structure II are hexadecahedra and 12 pentagons. The mean free diameter of this cavity is $\sim$ 6.7 ^{O}A.

When the effective diameter of the hydrate forming molecule (d_{eff}) < 5.1 ^{O}A, then a hydrate of structure I is formed in the presence of water. In principle, all of the eight cavities can be filled, e.g. hydrates of Ar, Xe, CH_4, H_2S, CO_2, etc. and consequently the ideal formula of this hydrate will be 8 M_1.46 H_2O or M_1.5.75 H_2O, where M_1 can be a molecule of Ar, Xe, CH_4, etc. If gas molecules larger than 5.8 ^{O}A but less than 6.9 ^{O}A in diameter are present, a type II structure crystalizes, e.g. hydrates of C_3H_8, iso-c_4H_{10}, $CHCl_3$, etc. The ideal formula of the hydrate will be 8 M_2.136 H_2O or M_2.17 H_2O, where M_2 can be a molecule of C_3H_8, $CHCl_3$, etc. The physical characteristics of each of the two hydrate structures are presented in Table 2.

3) Conditions for Formation of Hydrate

A clear presentation of the conditions of formation of

Table 2.   PHYSICAL PROPERTIES OF HYDRATE LATTICE

	Structure I	Structure II
No. of water molecules per unit cell	46	136
Number of cavities/unit cell		
small	2	16
large	6	8
Cavity radius, A^o		
small	3.94	3.91
large	4.30	4.73
Coordination No.		
small	20	20
large	24	28
Typical gases which form this structure	Methane	Propane
	Xenon	Iso-butane
	Argon	n-butane
	Krypton	Cyclopropane
	Ethane	
	Ethylene	
	Cyclopropane	

hydrates according to the equation $M + n H_2O \rightleftharpoons M.n H_2O$, can be obtained by considering the diagram in Figure 3. This figure may be used to represent the behavior of a gas which forms a hydrate in P-T coordinates on this diagram. Curve I characterizes the saturation vapor pressure of the hydrate-forming substance, P_M which in its turn is saturated with water vapor. Curve II represents the vapor pressure of the hydrate-forming substance M over the hydrate in the presence of liquid water. Curve II′ is the vapor pressure of M over the hydrate in the presence of ice. Curve III is the variation of the melting point of the hydrate to liquid with the pressure. Curve IV is the depression of the freezing point of water during the dissolution of M in it under pressure. In addition to a definite temperature and pressure, it is also required that a certain amount of water be present before any hydrate formation is possible. Water may be supplied as a vapor from the gas well. The gas is usually saturated with water vapor at the emergent temperature and pressure of the well so that any decrease in temperature or increase in pressure will cause some water vapor to liquefy and thus become a potential hydrate former.

Gas hydrates are not necessarily formed as soon as the proper conditions of pressure, temperature and composition are fulfilled. In one test (30) that was continued for a period of 40 hours, no gas hydrates were formed even though
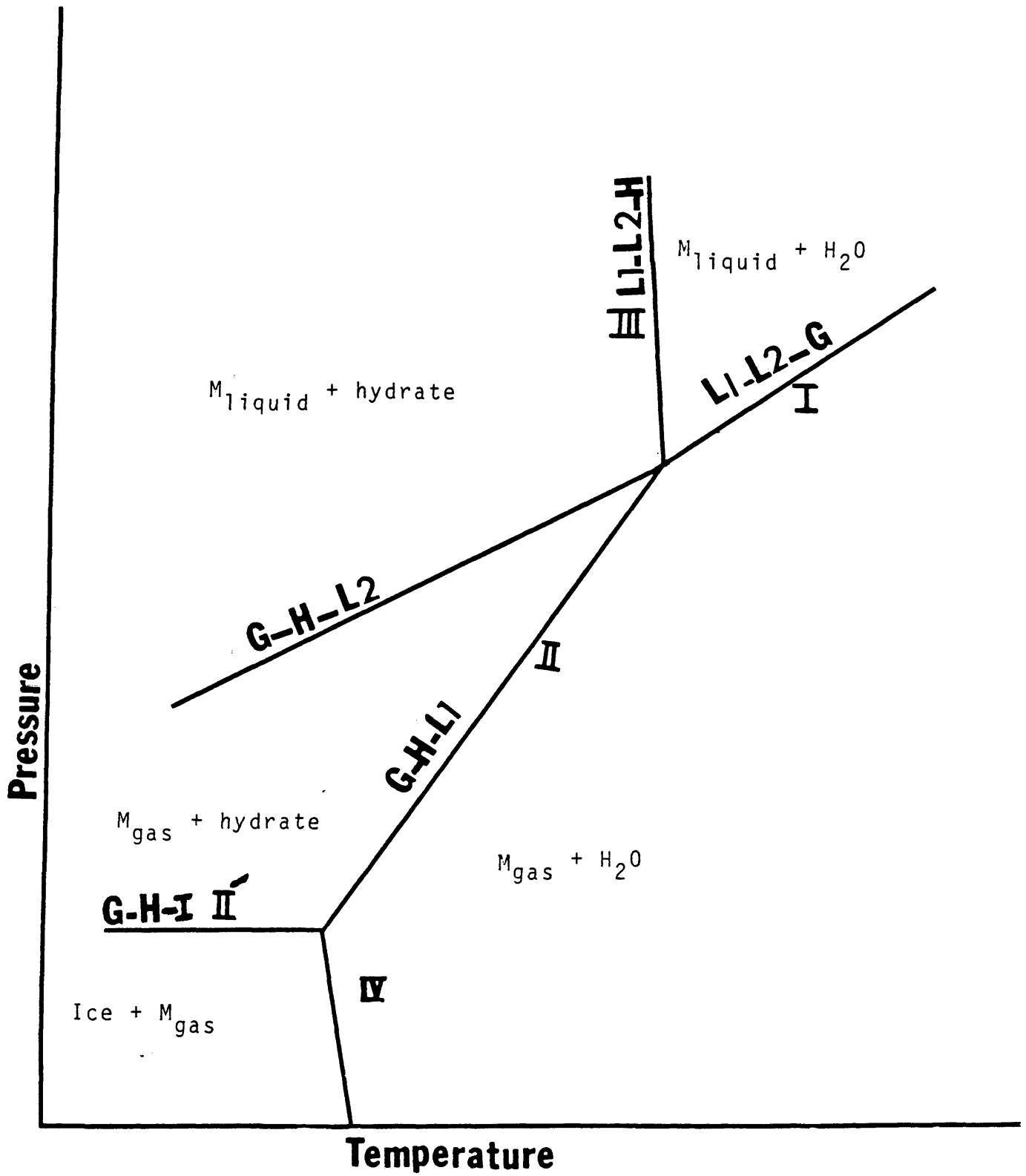
FIGURE 3.   PHASE DIAGRAM ILLUSTRATING HYDRATE FORMATION

the pressure and temperature and moisture content were such
that the existance of gas hydrates was entirely possible.
Unfortunately, this period of delay cannot be utilized in the
protection of gas lines against hydrate formation because
other factors such as the movement of the gas through the
line, pulsations caused by compressors, or anything that
might cause a stirring action within the system, tends to
destroy this period of delay and cause the immediate forma-
tion of the hydrate. The introduction of a crystal of the
hydrate will produce the same effect.

4) Determination of Hydrate Numbers

         The composition of the hydrate molecule, that is,
the ratio of gas to water in the molecule, can be calculated
from heats of formation of the hydrate from liquid water and
from ice. Since hydrates are nonstoichiometric,the value of
n depends upon the P-T-X condition at which it is measured.
Two direct methods of determining the composition of hydrates
are reported in the literature. The first method (31,32) the
amount of gas taken up by a known amount of water is volu-
metrically measured and the ratio of gas molecules to water
molecules is found by assuming all of the water is converted
to hydrate. A second method (33) involves nucleating hydra-
tes around a central cooling rod using silver iodide as a
crystal initiator. The hydrate phase is then separated and

analyzed. Unfortunately, both of these direct methods have experienced significant occulusion of water by the hydrate, making the accuracy of these methods questionable.

A third method, which is indirect, proceeds as follows: At a temperature of $32^\circ F$, the following equation can be written for the formation of hydrates of A:

$$nH_2O \ (1) + A \longrightarrow hydrate \qquad \Delta H_{liq} \qquad (4\text{-}1)$$

$$nH_2O \ (s) + A \longrightarrow hydrate \qquad \Delta H_s \qquad (4\text{-}2)$$

$$nH_2O \ (s) \longrightarrow (nH_2O)_{water} \quad \Delta H_f \qquad (4\text{-}3)$$
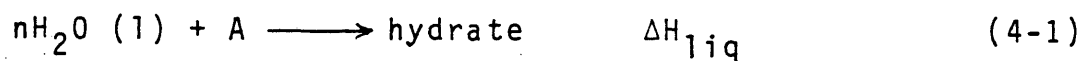
with the indicated enthalpy changes ΔH_{liq}, ΔH_s, ΔH_f. The following must hold:

$$\Delta H_f = \Delta H_s - \Delta H_{liq} \qquad (4\text{-}4)$$

In this equation, ΔH_f is just the latent heat of the freezing water, the enthalpy changes ΔH_{liq} and ΔH_s are found from P-T data using a modification of the Clapeyron equation

$$\frac{d(\ln P)}{dT} = \frac{\Delta H_{liq \ or \ s}}{ZRT^2} \qquad (4\text{-}5)$$

where Z is the compressibility factor. Hence, n can be determined by dividing ΔH_f by the molar latent heat of freezing for water. This method makes the assumption that the change in volume for hydrate formation is equal to the volume of gas enclathrated and that the water phase and hydrate phase compositions do not change with temperature.

5)   Recent Work in Hydrate Thermodynamics

As mentioned earlier, the x-ray diffraction work of
von Stackelberg and others enabled the determination of the
structure of gas hydrates and explained the non-stoichio-
metric nature of hydrates by suggesting fractional occupancy
of a cavity is just the fraction of all identical cavities
which have a gas molecule in them.

In 1959 Van der Waals developed a statistical thermo-
dynamic model of clathrate compounds which was able to pre-
dict the hydrate dissociation pressure of any mixture of
hydrate forming gases and water. The development incorpora-
ted the following basic assumptions (34):

1)   Each cavity in the hydrate has either one or zero
gas molecules in it. No double occupancy exists.

2)   The encaged gas molecule has the same rotational
freedom as it would in the gas phase. This means the cage
must be much larger in all dimensions than the largest
dimension of the gas molecule. For many molecules such as
propane and butane, this assumption is probably invalid.

3)   There is no solute-solute (gas-gas) interaction
within the hydrate, and the solute only interacts with its
nearest neighbor water molecules.

4)   The free energy contribution of the water molecule
is independent of the mode of dissolved gases.

5) A specific potential function accurately describes the water-solute interaction. For example, this function may be the spherical core Kihara potential or the Lennard Jones function.

The equation that resulted from this development is:

$$\Delta\mu_W^H = \mu_W^\beta - \mu_W^H = - RT \sum_m V_m \ln (1-\sum_j \theta mj) \qquad (5-1)$$

where $\Delta\mu^H$ is the difference between μ_W^β, the chemical potential of H_2O in the empty hydrate lattice and μ_W^H, the chemical potential in the filled hydrate lattice, R is the gas constant, and V_m is the number of cavities of type m per water molecule in the lattice. In the case of gas hydrates of structure I, $V_1 = 1/23$ and $V_2 = 3/23$; in the case of hydrate of structure II, $V_1 = 2/17$ and $V_2 = 1/17$ (35). The fraction of type m cavities occupied by gas componet 1 is given by

$$\theta_{m\ell} = C_{m\ell}f_\ell / (1 + \sum_j C_{mj}f_j) \qquad (5-2)$$

where $C_{m\ell}$ is the Langmuir constant which is a function of temperature and the potential function parameters, i.e.

C = C(T, σ, ε, a). Here σ is the molecular distance parameter, ε is the depth of the binary potential well, and a is the core radius of the gas molecule, using the Lennard-Jones-Devonshire cell theory. Van der Waals and

Platteeuw showed that the Langmuir constant is given by

$$C(T) = 4\pi/k \int_0^\infty \exp(-W(r)/kT) \, r^2 \, dr \qquad (5-3)$$

where $W(r)$ is the spherically symmetrical potential in the cavity, with r measured from the center. McKoy and Sinanoglu (36) derived $W(r)$ for spherical and line molecules of the Kihara potential. $W(r)$ is a function of the cell radius, the coordination number, Z, and the nature of the gas water interaction. The present work follows basically Parrish and Prausnitz's approach that showed an improvement over McKoy and Sinanoglu; i.e. $(\varepsilon/x)_{AB}$ and σAB that describes the host and guest molecules interactions were directly calculated from the equilibrium data along the ice-gas-hydrate, and water-gas-hydrate equilibrium line. Parrish and Prausnitz used Kihara potential which is slightly more accurate than the Lennard-Jones potentials used by Nagata and Kobayashi, (37,38). For two-components, equation (5-1) can be rewritten in terms of the Langmuir constants as the following

$$\Delta\mu^{\beta-H} = RT \sum_m V_m \ln(1 + \sum_j C_{ij} \, f_j) \qquad (5-4)$$

where f_j is the fugacity of the gas component j and given by the following equation.

$$f_j = \phi_j \, y_j \, P \qquad (5-5)$$

where ϕ_j is the fugacity coefficient of the gas component, y_j is the mole fraction in the gas phase of component j and P is the total pressure. At equilibrium, the chemical potential of H_2O in the hydrate phase equals that in each of the other coexisting phases. If ice is present,

$$\mu_W^H (T, P) = \mu_W^\alpha (T,P) \qquad (5\text{-}6)$$

where $\mu_W^\alpha (T,P)$ is the chemical potential of ice. If liquid water is present,

$$\mu_W^H (T, P) = \mu_W^L (T, P) + RT \ln X_W \qquad (5\text{-}7)$$

where $\mu_W^L (T, P)$ is the chemical potential of pure liquid water at T and P, and X_W is the mole fraction of water in the liquid phase. Sources of gas solubility data are given in reference (39).

Depending upon whether ice or liquid water is present, we define

$$\Delta\mu_W^\alpha = \mu_W^\beta - \mu_W^\alpha \qquad (5\text{-}8)$$

or

$$\Delta\mu_W^L = \mu_W^\beta - \mu_W^L \qquad (5\text{-}9)$$

Now equation (5-8) can be rewritten, if ice is present as

$$\Delta\mu_W^\alpha (T, P) = RT \sum_m V_m \ln (1 + \Sigma C_m f) \qquad (5\text{-}10)$$

or, if liquid water is present as

$$\Delta\mu_W^L (T, P) = RT \sum_m V_m \ln (1 + \Sigma C_m f) + RT \ln X_W \qquad (5\text{-}11)$$

The quantity $\Delta\mu_W^\alpha$ or $\Delta\mu_W^L$, when calculated from equation (5-10) or (5-11), is called the calculated chemical potential difference.

Parrish and Prausnitz (1972) calculated an experimental chemical potential difference $\Delta\mu_W^\alpha (T,P)$ or $\Delta\mu_W^L (T,P)$ using a reference hydrate in two steps (40).

1) For the reference hydrate, $\Delta\mu_W^\alpha (T, P_R)$ at the given temperature T, and reference hydrate dissociation pressure P_R, is found using

$$\Delta\mu_W^\alpha (T, P_R)/RT = \Delta\mu_W^\alpha (To, Po)/RTo - \int_{To}^{T} \frac{\Delta h_W^\alpha}{RT^2} dT$$

$$+ \int_{To}^{T} \left(\frac{\Delta v^\alpha}{RT}\right) (dP/dT) \, dT \qquad (5\text{-}12)$$

where Po is the dissociation pressure of the reference hydrate at the ice-point temperature To; Δh_W^α and Δv_W^α are, respectively, the molar difference in enthalpy and volume between the empty hydrate lattice and ice. Similarly, when

liquid water coexists with the hydrate,

$$\Delta\mu_W^L (T, P_R)/RT = \frac{\Delta\mu_W^L (To, Po)}{RTo} - \int_{To}^{T} \frac{(\Delta h_W^\alpha + \Delta h_W^f)}{RT^2} \, dT$$

$$+ \int_{To}^{T} \left[(\Delta v_W^\alpha + \Delta v_W^f)/RT \right] (dP/dT) \, dT \qquad (5\text{-}13)$$

where Δh_W^f and Δv_W^f are respectively, the molar difference in enthalpy and volume between ice and liquid water.

2) To obtain $\Delta\mu_W^\alpha$ at T and P, when ice is present we use

$$\Delta\mu_W^\alpha (T,P) = \Delta\mu_W^\alpha (T,P_R) + \Delta v^\alpha (P - P_R) \qquad (5\text{-}14)$$

and when liquid water is present:

$$\Delta\mu_W^L (T,P) = \Delta\mu_W^L (T,P_R) + (\Delta v_W^\alpha + \Delta v_W^f) (P - P_R) \qquad (5\text{-}15)$$

In the present study, since the liquid water is in equilibrium with the hydrate phase at a temperature above its ice point, the chemical potential difference given by equation (5-1) can be written as

$$\mu_W^H (T,P) = \mu_W^L (T,P) \qquad (5\text{-}16)$$

where $\mu_W^H (T,P)$, $\mu_W^L (T,P)$ are the chemical potential of hydrate and pure liquid water at the given temperature and pressure.

The chemical potential difference between water and the empty hydrate is calculated in a similar fashion (41).

$$\frac{\Delta \mu_W}{RT} = \frac{\Delta \mu_W^0}{RT_0} - \int_{T_0}^{T} \frac{\Delta h_W}{RT^2} \, dT + \int_{0}^{P} \frac{\Delta v_W}{RT} \, dP - \ln X_W \qquad (5\text{-}17)$$

The first term on the right is the reference chemical potential; the second term gives the temperature dependence at constant (zero) pressure. The third term corrects the pressure to the final equilibrium pressure. The last term corrects the chemical potential from that of a pure water or ice phase to that water-rich solution.

The temperature dependence of the enthalpy difference is given by

$$\Delta h_W = \Delta h_W^0 (T_0) + \int_{T_0}^{T} \Delta C_{PW} \, dT$$

where

$$\Delta C_{PW} = \Delta C_{PW}^0 (T_0) + b (T - T_0)$$

$$\Delta v_W = \Delta v_W^\alpha + \Delta v_W^f$$

The thermodynamic properties are given in Table 3.

6)   Predictive Techniques

The hydrate forming conditions could be predicted by the following ways:

a)   Early Predictive Technique

Katz and coworkers (42) showed that the hydrate forming conditions could be predicted using vapor-solid equilibrium constant analogus to vapor liquid equilibria. The equilibrium constants were determined from ternary mixture data by Kobayashi (1959) and corrected in GPA and API handbooks.

In this technique they determined that the conditions for initial hydrate formation are obtained by satisfying a relationship which is analogous to a dew point calculation for complex mixtures:

$$K_{v-s,i} = Y_i / X_i$$

where Y_i is the vapor phase mole fraction of the hydrate forming gas and X_i is the solid phase mole fraction of the same component on a water free basis. This method was not

used in this work because it does not distinguish between the two structures of hydrates.

b) Current Technique

Currently, many workers, in predicting the dissociation curve for various mixtures, use the Parrish and Prausnitz model (1972). The method is slightly more complex than the previous method, but it has the following advantages:

1) The equations are related to the hydrate structure, and 2) the theoretical nature of the model allows it to be extended beyond the gas (V)-liquid water (L)-hydrate (H) region.

The procedure for determining hydrate formation pressures for a given gas at a given temperature is as follows:

1) Guess a pressure.

2) At the guessed pressure, for the given temperature and gas mole fraction of component, determine the fugacity of component from an equation of state.

3) Using C_{mj} values from the Kihara potential and θ_{mj} values from step two, determine $\Delta\mu_W^H$ from equation (5-4).

4) Using constants from Table 3 , calculate $\Delta\mu_W^H$ from equation (5-17) at the temperature and guessed pressure.

Table 3.   <u>THERMODYNAMIC</u> <u>PROPERTIES</u> <u>OF</u> <u>EMPTY</u> <u>HYDRATE</u>
           <u>(β-PHASE)</u> <u>AND</u> <u>LIQUID</u> <u>WATER</u> <u>RELATIVE</u> <u>TO</u> <u>ICE</u>
           <u>(α-PHASE)</u> <u>AT</u> <u>0</u> <u>^{o}C</u> <u>AND</u> <u>ZERO</u> <u>PRESSURE</u>

	<u>Structure I</u>	<u>Structure II</u>
$\mu_W^\beta - \mu_W^\alpha$, cal/mole	310.0[a]	224.0[a]
$h_W^\beta - h_W^\alpha$, cal/mole	332.0[a]	245.0[a]
$V_W^\beta - V_W^\alpha$, cc/mole	3.0[b]	3.4[b]

ΔC_{PW}, cal/mol ^{o}K

$$T > To \qquad 9.11 - 0.0336 \, (T - To)^{[c]}$$

$$T < To \qquad 0.1349 - 0.00047 \, (T-To)^{[d]}$$

[a]Dharmawardhana, P. B., Ph. D. Thesis, CSM (49)

[b]Von Stackelberg and Müller (35)

[c]Weast (15)

[d]Holder, G. Corbin and K. D. Papadopoules (41).

5) If the values of $\Delta\mu$ in equation (5-4) and (5-17)
   are equal, then the P value is correct for hydrate
   formation; if not, guess a new value of P and
   return to Step 2.

7) Review of Experimental Data on Xenon-water Hydrate

The xenon-water hydrate has been the subject of study by
many investigators. The dissociation pressure of the xenon-
water hydrate has been measured experimentally above and below
$0^{\circ}C$. Early work was done by Forcrand (43), who placed xenon-
water in the equilibrium cell under pressure, and added a
piece of ice to the system, similar to "seeding" required to
form crystals. Godchot (44) did the same experiment in 1936
but he obtained different dissociation pressures. In 1939
Bernhard Braun (45) measured the dissociation pressure of
xenon hydrate at temperature from $0^{\circ}C$ to $20^{\circ}C$. The most
recent work was done by Ewing and Ionescu (46). The experi-
mental apparatus of the most recent work consisted of a gauge,
stainless-steel reaction vessel provided with a magnetic
stirrer, water pump, and a constant temperature bath. In
this experiment dissociation pressures were measured between
$0-20^{\circ}C$. About 17 ml of deionized water were placed in the
reaction vessel, and enough xenon was added to exceed the
solubility of xenon in water, then the system was allowed to

equilibrate at certain temperature. After the system equili-
briated (the pressure of xenon above the solution became
constant), a record was made for the pressure and the tempera-
ture.

The dissociation pressure of xenon-water below 0°C, was
measured by Barrer and Edge (47). The experimental appara-
tus consisted of a gas supply line and a volumetric sorption
system, reaction vessel. A charge of deionized water was
placed in the reaction vessel, and xenon gas was admitted to
the reaction vessel, then the system was allowed to reach
equilibrium at different temperature; then the pressure and
the temperature was recorded.

The most recent work was done by Miller (45). Miller
measured two sets of data on xenon-water hydrate (-67 to 0°C
and -99 to 0°C). The experimental apparatus consisted of
glass vacuum system with a mercury manometer, water bath and
measuring temperature system. In this experiment distilled
water was placed in the reaction vessel (glass vacuum system).
At each temperature the equilibrium dissociation pressure was
recorded.

The more recent work was done by D. W. Davidson (14).
Davidson measured the occupancy ratios of cages in xenon
hydrate at 273°K, directly from the NMR spectrum of the
129_{xe} isotope if the hydrate is made of D_2O rather than H_2O.

The θ's specify the degree of occupancy of the small and large cages. The degree of occupancy of each kind of cage is related to the pressure by a Langmuir equation like equation (5-2). One can calculate the Langmuir constants from some model of the potential of intermolecular forces between the encaged molecule and the water molecules which constitutes the cage. This is commonly done by adapting the Lennard-Jones-Devonshire spherical cell model for liquids to the hydrate case: the cage water molecules are smeared out to form a uniform spherical surface and the interaction described by Kihara 12-6 potential function. Since Langmuir constants can be calculated for larger and smaller cage type, then the occupancy ratios of cages can be calculated for comparison with those of Davidson which were determined by NMR.

THE EXPERIMENTAL APPARATUS AND PROCEDURE

I)   The Experimental Apparatus

The pressure, temperature at which hydrates formed were measured for xenon-water, using equipment which was very similar to that used by many previous investigators (48,49 50).

The schematic diagram of the experimental system is shown in Fig. 4.   The description of the apparatus is presented under the following subsections.

   a)   The equilibrium cell,

   b)   The pressure measuring system,

   c)   The temperature measuring system and the associated control system,

   d)   The agitation and vacuum system,

   e)   The gas charging system,

   f)   The liquid charging system.

a)   The Equilibrium Cell

The equilibrium cell as illustrated in figures 5 and 6, is a cylindrical cell in which hydrates are measured.   The cell dimensions were: 2 inch I.D. cylindrical bore and 5 inches long.   It was constructed of a bearing bronze alloy (83% cu, 7% tin, 7% lead, 3% zinc), with a tensile strength of 40,000 psia.   The design pressure was in excess of 1,000 psia for an operating temperature from $-22^{\circ}F$ to $212^{\circ}F$.
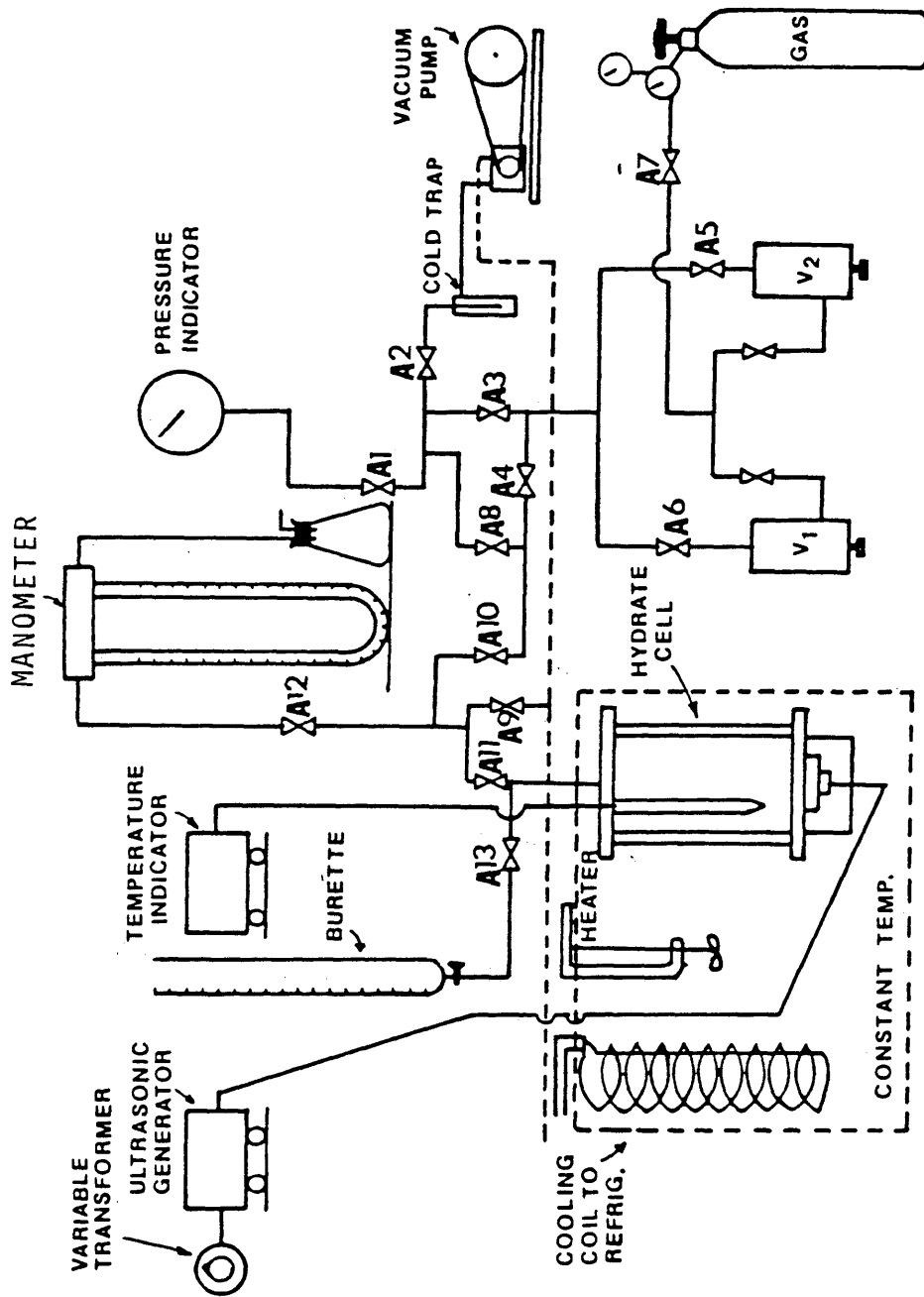
FIGURE 4. EXPERIMENTAL APPARATUS
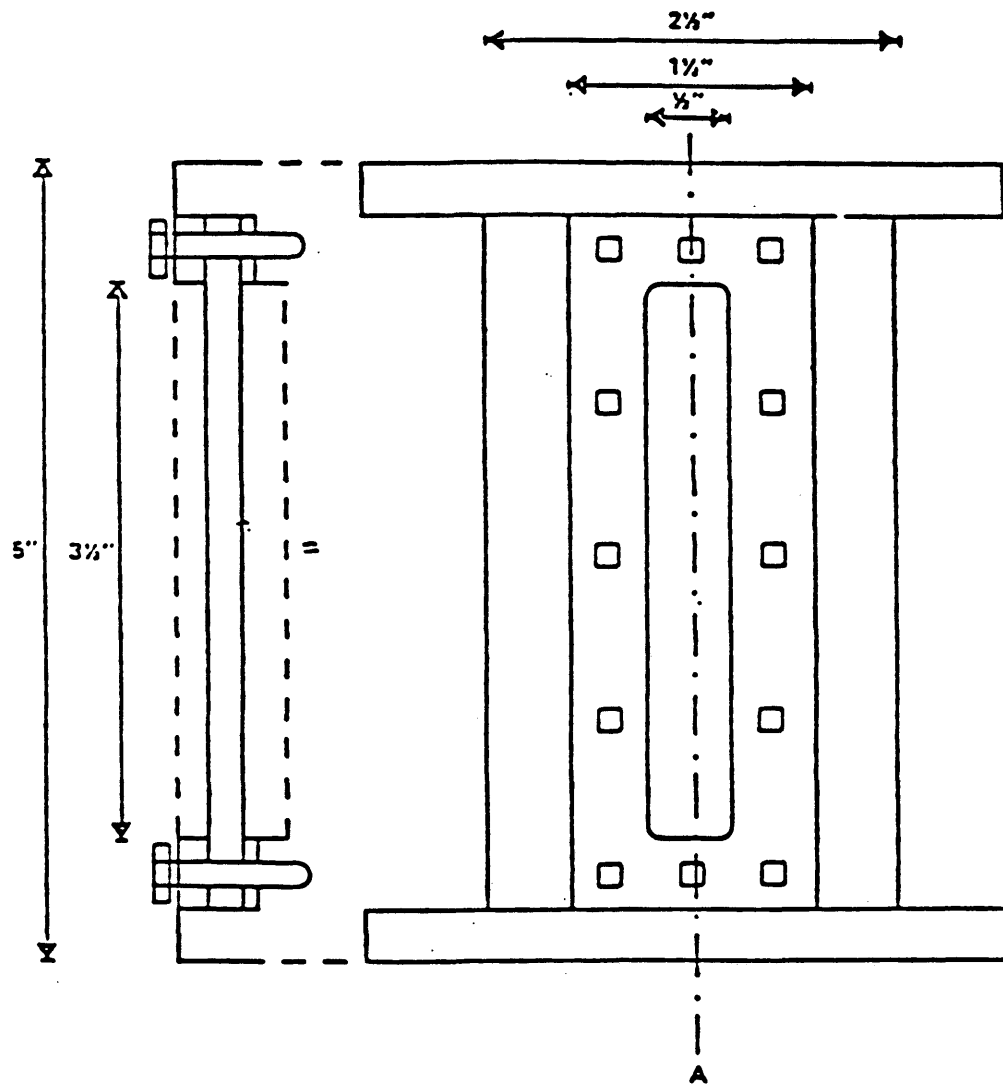
FIGURE 5.   SCHEMATIC DRAWING OF THE EQUILIBRIUM
            CELL WINDOWS (TAKEN FROM ZERPA (48)).

1 Gas inlet

2 Conductivity probe

3 Platinum resistance
   themometer

4 Cooling coil

5 Shell of the eq.
   cell

6 "O" ring

7 Ultrasonic trans-
   ducer

8 Aluminum covering
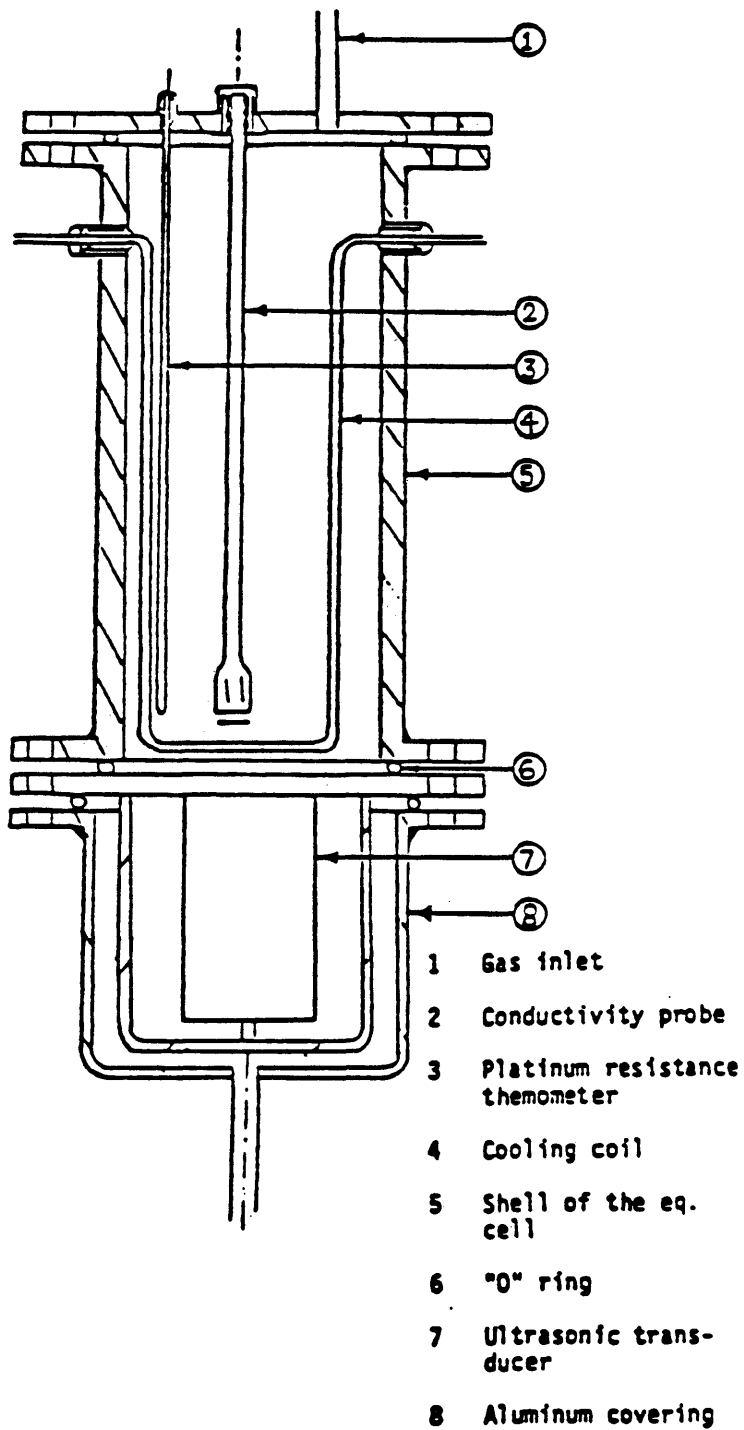
FIGURE 6.   THE EQUILIBRIUM CELL (TAKEN FROM ZERPA (48)).

Closures on the cell were made of type 410 stainless steel.
Each closure was removable and was attached with six 3/8
inch bolts. Rubber "O" ring gaskets were used as seals on
the top and bottom closures. Two sight glass windows were
built on opposite sides of the cell in order to observe the
hydrate formation. The windows were 1/4 inch plexiglass
with teflon gasket seals. Each window was attached with
twelve 1.8 inch bolts. The ultrasonic transducer that pro-
duced agitation of the liquid in the cell was bolted to the
outside of the lower plate. This was covered by a 3 inch
I.D. aluminum cover. The cell was connected to the gas and
water charging system through a 1/4 inch tube attached to
the top plate. The platinum resistance thermometer was
attached to the top plate of the cell by an Omega lock
compression fitting. The equilibrium cell was supported
by three legs of 4.5 inch long inside a 127 cubic inch rec-
tangular box, constructed mainly for bath fluid displacement.

b) The Pressure Measuring System

The pressure measuring system consisted of a Heise Gauge,
and a manometer and the tubing which connected the gauge with
the equilibrium cell. The pressure gauge was a Bourdon tube
gauge Model CM from Dresser Industries, which is intended
for absolute pressure measurements. The Heise gauge was
calibrated against Ruska air dead weight tester. The results

of the calibrations are given in Appendix A. The connect-
ing tubing between the gauge and the cell was commercial
1/4 inch copper tubing.

c) The Temperature Measuring System and the Associated
    Control System.

The temperature in the cell was sensed by a 5.5 inch long
Omega, type PR-13 platinum resistance temperature probe. The
temperature was read by a digital readout Model 199 P1 from
Omega. The temperature range was from -200 ^{o}C to -800 ^{o}C
with a conformity ± 1 count (maximma). The platinum resis-
tance and readout systems were calibrated against a Müeller
temperature bridge. The results of calibrations are given
in Appendix A.

The temperature bath was constructed of 0.5 inch plexi-
glas sheets. The dimensions of the bath were as follows;
13 inch in length, 7.5 inches in width, 17 inches in height
with an overall capacity of 5.5 gallons. The outer wall of
the bath was insulated with 1 inch thick Amofex foam sheets.
The bath fluid was Dow-Corning 200 silicone fluid with a
freezing point of -40 ^{o}F and viscosity of 5 centistokes.
This fluid was selected mainly because of its good dielec-
tric properties.

The refrigeration system was Model Pcc-24A-3 Blue M
Hermatic refrigerator 1/2 HP compressor with an overall

heat removable capacity of 3500 Btu/hr. The temperature range was $-23^{\circ}C$ to room temperature with the temperature control within $\pm 0.15\ ^{\circ}C$. The refrigerant Freon-12 emerged through a thermostatic expansion valve and flowed through a stainless steel coil of 7/16 inch O.D. wound on a 7 inch mandrel. The refrigerator was equipped with a hot gas by-pass system to minimize under shooting and to allow better control of the cooling. The temperature of the bath was further controlled by a Model 1440-GKU Thermomix controller. from VWR Scientific with a built in immersed thermostat of 750 watt capacity and a 10 liter/min capacity circulating pump. With the thermomix controller and the Blue M refrigerator the temperature of the bath was controlled within $+ 0.005\ ^{\circ}C$ at a temperature range at $0\ ^{\circ}C$ to $10\ ^{\circ}C$.

d) The Agitation and Vacuum System

The ultrasonic agitation system consisted of an ultrasonic transducer attached to the bottom plate of the equilibrium cell and connected to an ultrasonic generator with a 25 foot leak proof cable. The transducer assembly consisted of a steel back block, a pair of lead zirconate titanate ferroelectric elements with a connector tab and an aluminum front block.

The ultrasonic generator was a solid-state module which operated from a commercial 120 V, 60 HZ electrical outlet.

The generator allowed the resonant frequency of the dynamic

unit to control the generator and it is usually operated

at about 24.5 KHZ. The maximum power output was 75 watts. ·

The power input to the ultrasonic system was regulated by a

variac. The ultrasonic unit was assembled by Bliss Sonic

Company in Fayetteville, Pennsylvania. The ultrasonic sys-

tem was designed for an optimum efficiency with 2.5 inches

of liquid in the cell.

The vacuum system consisted of a vacuum pump, which was

connected to the equilibrium cell via 1/4 inch copper tubing

through the manometer.

The liquid acetone cold trap was used on the up stream

of the pump to prevent any condensibles from entering the

pump and back diffusion of the pump oil. The outlet of the

pump was vented to the atmosphere outside the building.

e)   The Gas Charging System

The gas charging system consists of a size D xenon

cylinder, one volumetric volumeter and an assembly of valves

and tubing connected to the equilibrium cell. The gas

regulator had a delivery pressure of 200 psi. The gas

analysis which was provided by Union Carbide Corporation,

Linde Division, was as follows:

Material	Purity
Ar	< 1 ppm
CO_2	< 1 ppm
TH_c	< 2 ppm
H_2	< 1 ppm
O_2	< 1 ppm
Kr	< 25 ppm
CHu	< 1 ppm
H_2O	< 3 ppm
Ne	< 1 ppm
N_2	< 5 ppm

The gas was analyzed chromatographically and found to be 99.99% pure Xenon (0.01% krypton).

f) The Liquid Charging System

The water solution was charged to the evacuated cell from the 250 ml buret with graduations of 1.0 ml. The buret was open to the atmosphere and connected to a bellows seal valve and tubing assembly by approximately six inches of 1/4 inch Tygon tubing. The remaining tubing throughout the entire experimental apparatus was 1/4 inch copper tubing. The valves of the assembly were commercial, 1/4 inch NUPRO B-4H bellows valves. All of the valves in the system were the same.

II) Procedure

The procedure was, in general, to determine the dissociation pressure of xenon hydrate above 0 ^{o}C.

The procedure followed in obtaining data:

1. Initially, the equilibrium cell was thoroughly cleaned and dried.

2. The bottom part of the equilibrium cell, i.e. the ultrasonic system, bottom cell plate and the legs were connnected to the shell of the equilibrium cell.

3. The cell was submerged in the bath and connected to the liquid and gas charging system. The cell was then evacuated and pressurized to about 90 psia with helium for leak checks.

4. The valves A1, A5, A6, were kept closed. The valves A2, A3, A4, A8, A9, A10, A11, and A12 all were opened and the system was evacuated overnight.

5. Gas inlet valve A11 was closed. Two hundred milliliters of double distilled water (CO_2 free) were then charged to the evacuated cell from the 250 milliliter buret through the liquid feed valve A13. Then the cell was evacuated again for small intervals of time.

6. After determining the temperature at which the first run would be made, the thermocontrol was set and the system was cooled down by the refrigeration coils in the bath until the set point temperature of the thermocontrol is reached.

7. When the cell and all connecting tubing had been thoroughly evacuated, xenon was admitted to the system through the volumeter. The pressure admitted was estimated to be slightly higher than the expected hydrate formation pressure, similar to the "seeding" required to form crystals. This initial pressure was recorded when forming hydrates. The ultrasonic generator was then turned on for good mixing. After the hydrates had formed, a process requiring roughly seven hours, the ultrasonic agitation was stopped because temperature control to 0.02 $^{\circ}$C was not possible with the ultrasonic generator on.

8. The system was allowed to reach equilibrium, and then pressure and temperature were recorded. Then the temperature control was set to a different temperature for the next data point.

EXPERIMENTAL RESULTS

The main aim in the present work was to determine the dissociation pressure of xenon-water in the temperature range of 273-283°K. These experimental values vary considerably from those determined by other investigators. The experimental results given in Table 4, were compared with calculated values in Figure 7. The solid line was generated from the computer program HYDXEN.FOR, which can be found in Appendix B. This program is based on the Parrish-Prausnitz model using parameters of Dharmawardhana, et al. (1980). The data was also fit with a stepwise multiple linear regression program, and the following equation for the xenon hydrate above 273°K resulted:

$$\ln P = 33.311993 - \frac{8257.082}{T}$$

where P is the dissociation pressures predicted in psia.

T is the corresponding dissociation temperature in °K.

TABLE 4

DATA OF XENON HYDRATE OF THE PRESENT STUDY

$T\,^oF$	P_{exp}(psia)	P_{cal}(psia)	Difference (%)
32.0	22.1	21.9	0.9
33.6	24.0	24.0	0.0
34.7	25.6	25.8	0.7
36.5	28.8	28.8	0.0
37.9	31.2	31.2	0.0
39.4	34.3	34.2	0.3
41.0	37.8	37.6	0.5
41.9	39.6	39.6	0.0
43.2	42.6	42.6	0.0
44.1	45.0	45.0	0.0
45.3	48.5	48.5	0.0
46.6	52.2	52.2	0.0
47.5	55.0	55.0	0.0
48.6	58.7	58.7	0.0
50.0	63.7	63.7	0.0

$\Delta\mu(0,0)$ cal/gmol   = 310.0

ϵ/k ^oK = 188.0

σ ^oA =   3.48299

a ^oA =   0.2098
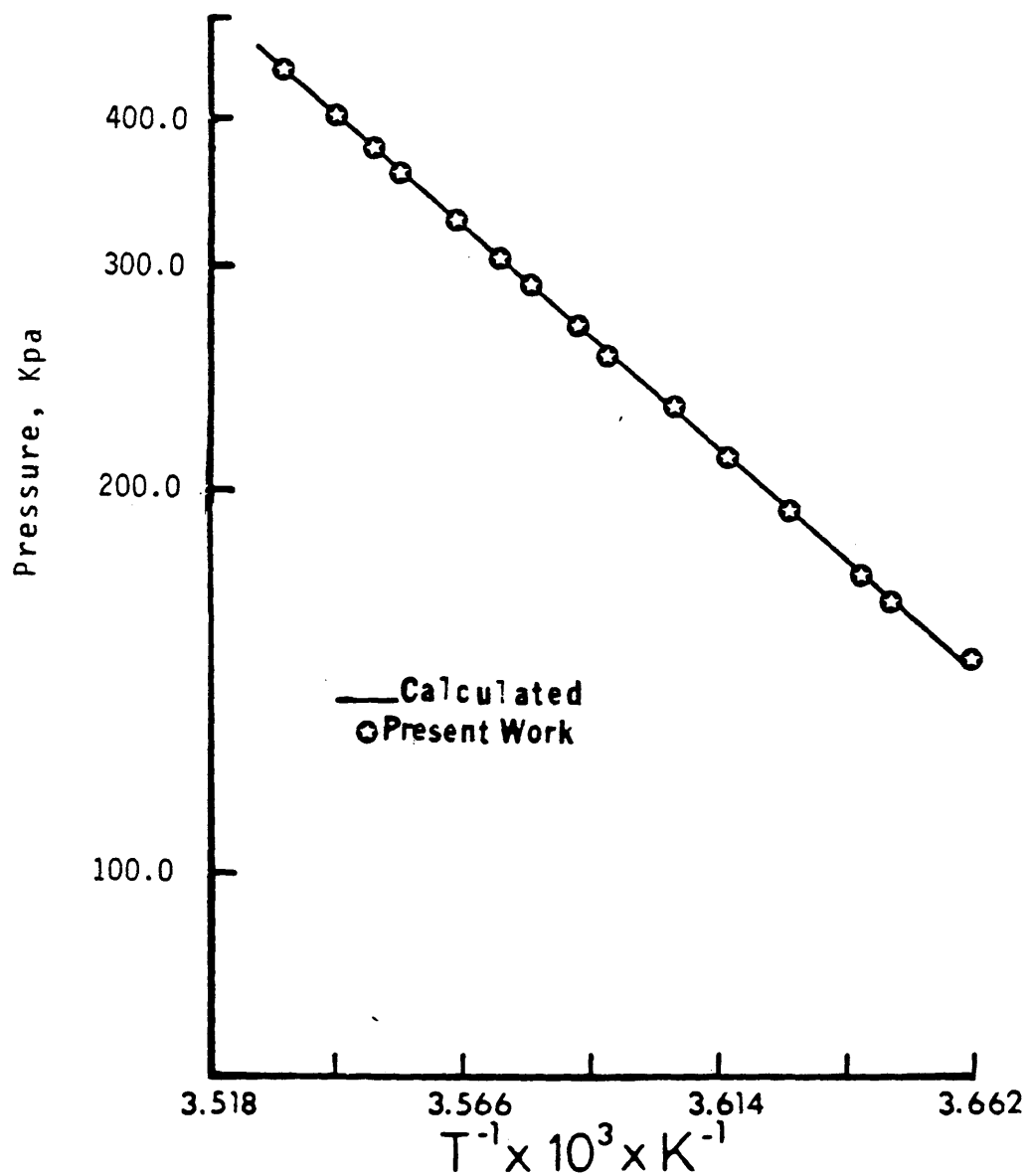
FIGURE 7.

PRESENT WORK ON XENON HYDRATE WITH
CALCULATED VALUES.

DISCUSSION

The object of this study was to find a better dissocia-
tion pressure curve for xenon hydrate. These data, along
with those of Miller below 273°K, were used to obtain better
Kihara parameters for the solid hydrate model.

The result of the experiment with other investigators
data are given in Appendix B, and presented graphically in
Figure 8. In this figure the calculated values are given
by the solid line. The data of the present work are in
good agreement with those values calculated from the theo-
retical model.

At the conclusion of this work, but before the final
thesis defense, Professor C. J. Peters, of the Delft
University of Technology, gave this laboratory the thesis
of L. Aaldijk, which was done in 1971 on xenon hydrates,
but never published. The xenon data of Aaldijk is also
shown in Figure 8. As may be seen, the comparison with the
data of the present work is excellent.

It is clear from the literature review that the $\Delta\mu^{\beta-\alpha}_{T,P}$
along the three-phase line, could be evaluated in two inde-
pendent routes such as: by knowing $\Delta\mu^{\beta-\alpha}_{0,0}$ $\Delta h^{\beta-\alpha}_{0,0}$, from
Dharmawardhana (1980), and the equilibrium temperatures and
pressures one could evaluate $\Delta\mu^{\beta-H}_{T,P}$ using the thermodynamic
model of Parrish-Prausnitz, equation (5-13) and (5-14).

However in this study the equation given by G. D. Holder
(5-17) was used, and by knowing the Kihara parameters,
equilibrium temperature and pressure one could evaluate
$\Delta\mu_{T,P}^{\beta-H}$ using the Van Der Waals and Plateeuw's model,
equation (5-1, 5-2, and 5-3).

Therefore with the right set of Kihara parameters,
$\Delta\mu_{T,P}^{\beta-H}$ calculated from the two routes by using equations
(a) (5-17) and (b) (5-11) should coincide. This concept
was used in optimizing the Kihara parameters. The core
diameters of the guest molecules were obtained from the
work of Tee, et al. (3). Hence the optimization was done on
ε/k and σ only.

The Kihara parameters were calculated using Miller's
data below $273^{O}K$. These data were used in a stepwise
multiple linear regression program, and the following
equation resulted:

$$\ln P = 25.986881 - \frac{3531.023}{T} - 1.763631 \ln T$$

where P is the dissociation pressure for xenon hydrate
below $273^{O}K$, and T is the corresponding temperature in ^{O}K
less than $273^{O}K$. Miller obtained two sets of data which
agree with each other very well. Miller's data also agree
with the dissociation pressure calculated using the computer
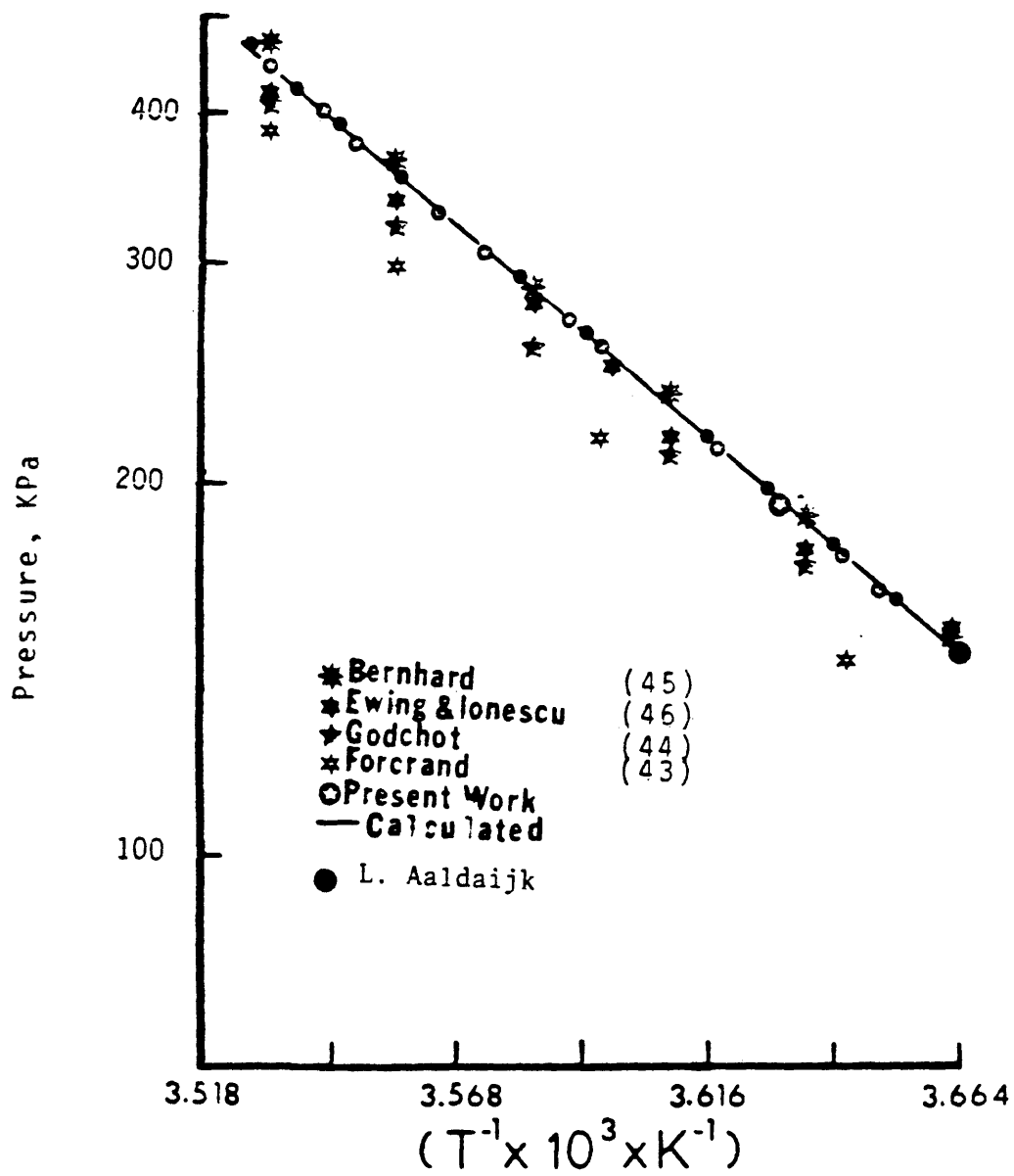
FIGURE 8

XENON HYDRATE DATA AND THE CALCULATED VALUES

model as shown in Figure 9.

The Kihara parameters obtained from Miller's data below 273°K, were used to predict the data of the present work above 273°K and are seen in Figure 7. In this figure, the predicted values are given as a solid line.

In this work the occupancy ratios of cages in xenon-water hydrate at 273°K were calculated. The degree of occupancy of each kind of cage is related to the gas fugacity by a Langmuir equation. In principle, one can attempt to calculate the Langmuir constants from some model of potential of intermolecular force between the encaged molecule and the water molecules which constitute the cage. Since the Langmuir constants were calculated the degree of occupancy of the small and large cages can be obtained by using the Langmuir equation, and the ratio of cages in water-xenon hydrate (θ_L/θ_S) at 273°K was calculated. This ratio was calculated with different values of $\Delta\mu_{0,0}^{\beta-\alpha}$ and the results obtained are given in Table 5.

The Davidson value of θ_L/θ_S at 273°K is equal to 1.30, determined by NMR measurement, seems to compare with a $\Delta\nu_{0,0}^{\beta-\alpha}$ of 304 cal/gmol by linear intrapolation from Table 6. Also from Table 6 it appears that the Dharmawardhana, Parrish and Sloan (1980) value of $\Delta\mu_{0,0}$ equal 310 cal/gmol is most successful in fitting the data, and corresponds
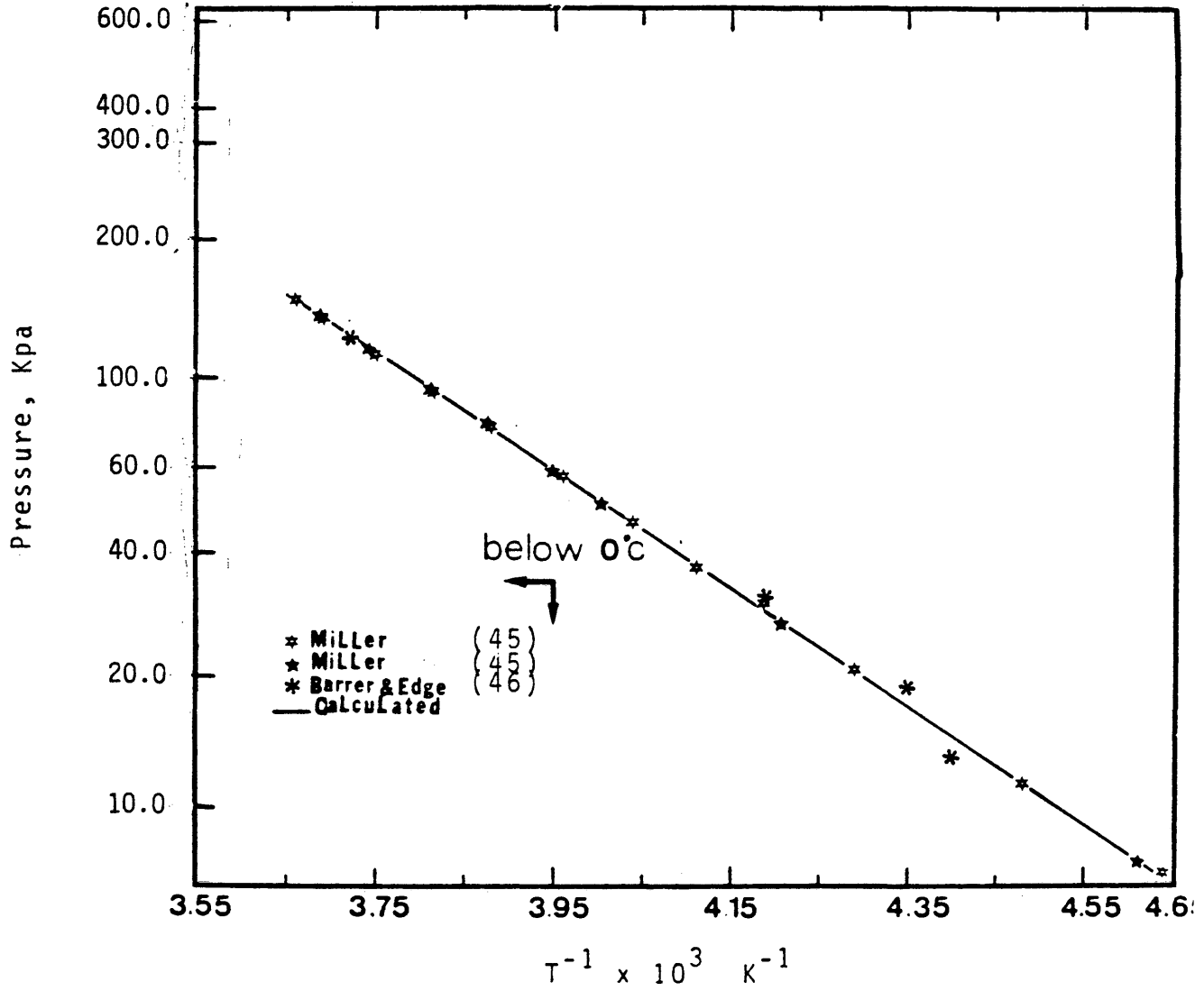
FIGURE 9.

. XENON HYDRATE DATA BELOW 273 $^{\circ}$K WITH THE CALCULATED VALUES

to θ_L/θ_S equal to 1.15. This is 11.5% different from the NMR value; also the results of the present value of θ_L/θ_S are better than the other investigators values as given in Table 5.

Davidson suggests that a new potential function such as that which is given by Meath (51) could give a close fit between $\Delta\mu_{0,0}^{\beta-\alpha}$ and θ_L/θ_S values.

The values of θ_L, θ_S, $\Delta\mu_{0,0}$ and the ratio of θ_L/θ_S are given in Table 7. By referring to Table 7 and Appendix C one can clearly notice the difference between the experimental and the theoretical values. The "NMR Experimental" values in Table 7 and Appendix C were obtained from Davidson's NMR values combined with values of water molecules/xenon molecule in the hydrate (M) from the experiment. The values of n were obtained using equation (4-5) as indicated on Page 17. The reasons for this difference are:

A. The determined NMR data is based on D_2O at $0^{\circ}C$ instead of H_2O at the same condition. That these data should be different is shown by Figure 10. The data of Figure 10 is obtained from cyclopropane hydrate based on both D_2O and H_2O. The data of cyclopropane hydrate is obtained from the work of Hafemann and Miller (52, 53).

B. The range of ε/k, over which we attempted to fit

TABLE 5. CALCULATED OCCUPANCY RATIOS OF CAGES IN XENON HYDRATE AT 273°K

Authors	Method	$\Delta\mu$(cal/mole H$_2$O)	n	a_L/a_S
van der Waals & Platteeuw (34)	Lennard-Jones-Devonshire; cell; 12-6 potential	167	6.93	1.027
Davidson (14)	Same	265	6.12	0.978
Parrish & Prausnitz (15)	L-J-D cell; 12-6 potential with spherical core	302	6.08	1.038
Tester, Bivins & Herrick (14)	Monte Carlo treatment of 12-6 pair-wise interactions	302	6.01	0.988
Ritmeester & Davidson (14)	Experiment: 129xe NMR			1.30 ± 0.03
Present Study	L-J-D cell; 12-6 potential with spherical core	310.0	6.90	1.15

Where

$\Delta\mu$ is the assumed excess free energy of water in the empty hydrate over its value in ice; n is the calculated number of water molecules per xenon atom in the equilibrium hydrate.

TABLE 6. CALCULATION OF DISSOCIATION PRESSURE AT DIFFERENT VALUES OF $\Delta\mu_{0,0}$ CAL/GMOLE

$\Delta\mu_{0,0}$ cal/gmole	302.0		305.0		310.0		315.0		320.0	
ϵ/k	186.0		187.0		188.0		189.0		190.0	
$\sigma\ ^{\circ}A$	3.47799		3.49299		3.48299		3.47099		3.46099	
θ_L/θ_S	1.58		1.21		1.15		1.10		1.08	
P_{ex} Psia	P_{cal} Psia	$(\frac{P_{ex}-P_{cal}}{P_{cal}})100$	P_{cal} Psia	$(\frac{P_{ex}-P_{cal}}{P_{cal}})100$	P_{cal} Psia	$(\frac{P_{ex}-P_{cal}}{P_{cal}})100$	P_{cal} Psia	$(\frac{P_{ex}-P_{cal}}{P_{cal}})100$	P_{cal} Psia	$(\frac{P_{ex}-P_{cal}}{P_{cal}})100$
22.1	22.0	0.45	21.9	0.9	21.9	0.9	22.0	0.45	22.1	0
24.0	24.3	1.2	24.0	0	24.0	0	24.2	0.8	24.2	0.8
25.6	26.1	1.9	25.8	0.7	25.8	0.7	25.8	0.7	25.8	0.7
28.8	29.2	1.4	28.8	0	28.8	0	28.8	0	28.8	0
31.2	31.9	2.2	31.2	0	31.2	0	31.2	0	31.2	0
34.3	35.0	2.0	34.3	0	34.2	0	34.1	0.5	34.0	0.8
37.8	38.7	2.4	37.8	0	37.6	0.5	37.4	1.0	37.3	1.3
39.6	40.9	3.3	39.9	0.7	39.6	0	39.6	0	39.3	0.7
42.6	44.3	3.9	43.1	1.1	42.6	0	42.6	0	42.3	0.7
45.0	46.9	4.2	45.5	1.1	45.0	0	45.0	0	44.5	1.1
48.5	50.5	4.1	48.8	0.6	48.5	0	48.1	0.8	47.7	1.6
52.2	54.7	4.7	52.7	0.9	52.2	0	51.8	0.7	51.4	1.5
55.0	57.8	5.0	55.6	1.0	55.0	0	54.6	0	54.1	1.6
58.7	61.6	4.9	59.4	1.2	58.7	0	58.2	0.8	57.6	1.8
63.7	67.4	5.8	64.5	1.2	63.7	0	63.7	0	62.4	2.0
X	3.04		0.62		0.14		0.38		0.97	

the data was 170-303, for sigma the range was 3.19-3.35
and for $\Delta\mu_{0,0}$ the range was 175-310. Tables 8 and 9
illustrate the values of ε/k, σ and $\Delta\mu_{0,0}$ which fit the
data best.

According to the above discussion, it is suggested
that the dissociation pressure of xenon should be obtained
based on D_2O at $0^{o}C$ instead of H_2O at the same condition,
if a comparison to Davidson's NMR results is to be made,
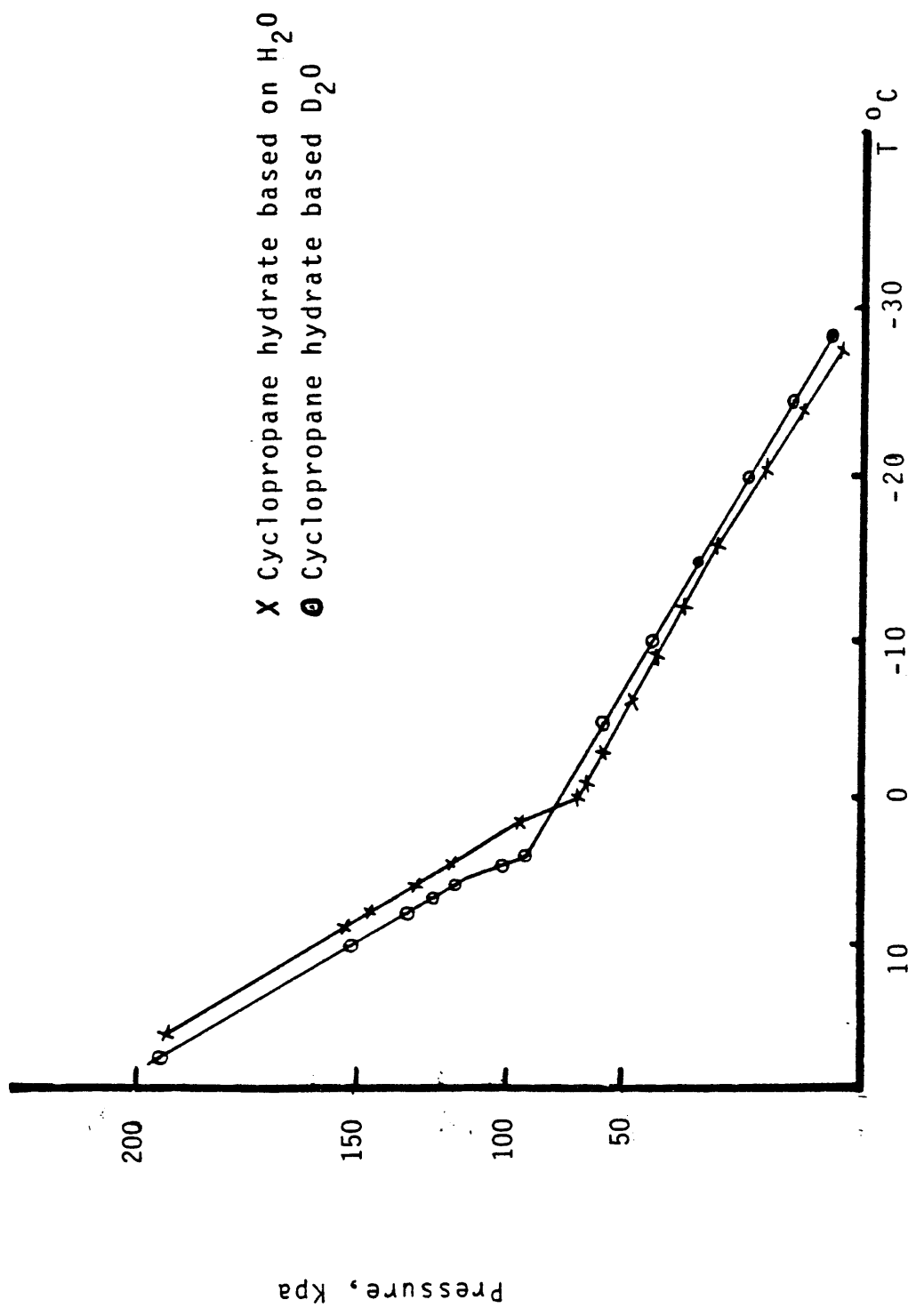
FIGURE 10. CYCLOPROPANE HYDRATE DATA BASED ON H_2O AND D_2O.

TABLE 7.   COMPARISON BETWEEN NMR AND THE   THEORETICAL VALUES
OF θ_L, θ_S, AND $\Delta\mu_{0,0}$

	NMR Exp.	Theroetical
C_{ml}	4.92	44.55
C_{ms}	1.417	0.2527
$\Delta\mu_{0,0}$ cal/gmol	175.8	304.0
C_{ml}/C_{ms}	1.3	1.15

FIGURE 8. CALCULATION OF DISSOCIATION PRESSURE BELOW 0°C AT DIFFERENT VALUES OF ε/K AND σ AT CONSTANT $\Delta\mu_{0,0}$ EQUAL TO 310.0 CAL/GMOL

ε/K	193.0		200.0		2.03	
σ °A	3.35		3.27		3.1906	
ϵ_L/ϵ_S	1.16		1.054		1.043	
Pex. Psia	P_{cal} Psia	$(\frac{P_{ex}-P_{cal}}{P_{ex}})100$	P_{cal}	$(\frac{P_{ex}-P_{cal}}{P_{ex}})100$	P_{cal} Psia	$(\frac{P_{ex}-P_{cal}}{P_{ex}})100$
21.8	21.8	0.0	22.1	1.3	21.4	1.8
19.7	19.7	0.0	20.1	1.9	19.4	1.5
16.4	16.5	0.6	16.9	3.0	16.3	0.6
13.5	13.8	0.2	14.2	5.2	13.7	1.4
11.1	11.4	2.6	11.8	5.9	11.3	1.7
8.6	8.9	3.4	9.3	7.5	9.0	44.4
6.7	7.0	4.3	7.4	9.4	7.1	5.6
5.3	5.6	5.3	5.9	10.2	5.7	7.0
4.4	4.6	4.3	4.9	10.2	4.7	6.4
3.1	3.3	6.1	3.6	13.8	3.4	2.6
2.3	2.5	8.0	2.7	14.8	2.6	11.5
1.2	1.9	36.8	2.1	42.8	2.0	40.0
1.0	1.2	16.6	1.3	23.0	1.2	16.6
0.6	0.8	25.0	0.9	33.3	0.8	25.0
0.4	0.5	20.0	0.6	33.3	0.5	20.0
0.2	0.3	33.33	0.3	33.3	0.3	33.3
0.2	0.2	0.0	0.2	0.0	0.2	0.0
0.1	0.1	0.0	0.2	50.0	0.2	50.0

FIGURE 9. CALCULATION OF DISSOCIATION PRESSURE ABOVE
0°C AT DIFFERENT VALUES OF ϵ/K AND σ AT
CONSTANT $\Delta\mu_{0,0}$ EQUAL TO 310.0 CAL/GMOL

$\epsilon/10$	193.0			200.0		203.03	
σ A$^\circ$	3.35			3.27		3.2906	
ϵ_L/ϵ_S	1.16			1.054		1.043	
$P_{ex.}$ Psia	P_{cal} Psia	$(\frac{P_{ex}-P_{cal}}{P_{ex}})100$		P_{cal} Psia	$(\frac{P_{ex}-P_{cal}}{P_{ex}})100$	P_{cal} Psia	$(\frac{P_{ex}-P_{cal}}{P_{ex.}})100$
22.1	21.8	1.3		22.1	0.0	21.3	3.6
24.0	23.8	0.8		24.0	0.0	23.3	2.9
25.6	25.2	1.5		25.6	0.0	24.6	3.9
28.8	27.8	3.4		28.1	2.4	27.1	5.9
31.2	30.0	3.8		30.3	2.8	29.2	6.4
34.3	32.5	5.2		32.7	4.6	31.5	8.8
37.8	35.4	6.3		35.6	5.3	34.4	•8.9
39.6	37.2	6.1		37.3	5.8	36.1	8.8
42.6	39.9	6.3		40.0	6.1	38.7	9.1
45.0	41.8	7.1		41.9	6.8	40.5	10.0
48.5	44.5	8.2		44.5	8.2	43.2	10.9
52.2	47.7	8.6		47.6	8.8	46.2	11.5
55.0	50.1	8.9		50.2	8.7	51.3	6.7
58.7	53.3	9.2		53.1	9.5	48.5	17.4
63.7	57.4	9.8		57.2	10.2	55.2	13.3

CONCLUSIONS

1) Data for xenon-water hydrate dissociation pressure were obtained between $273^{O}K$ and $183^{O}K$.

2) Using Dharmawardhana's values for $\Delta\mu_{0,0}$, and $\Delta h_{0,0}$, Kihara parameters were obtained to give good fits to the data of Miller and the data of the present work.

3) The occupancy ratio of cages in xenon hydrate at $273^{O}K$ was calculated and found to agree within 11% with the NMR obtained ratio. The discrepancy was explained by the fact that the NMR data used D_2O instead of water.

RECOMMENDATIONS

1) It is recommended that xenon hydrate dissociation data be obtained at temperature higher than $283^{\circ}K$ to expand the data range.

2) It is recommended that a new potential function, such as that by Meath, et al. be used to describe the guest-cage interaction for hydrates.

3) It is recommended that xenon hydrate dissociation data be obtained based on D_2O to get a better comparison with the NMR data of Davidson.

NOMENCLATURE

a	=	core radius, $^{\circ}A$
C_m	=	Langmuir constant for component ℓ in cavity m, at m^{-1}
f_ℓ	=	fugacity of component ℓ , atm
n	=	number of mole
h_W^α, h_W^β	=	molar enthalpy of pure ice and empty hydrate lattice, respectively, cal/mole
K	=	Boltzmann's constnat, 1.38×10^{-16} erg/$^{\circ}K$
P	=	total pressure, atm
P_o	=	dissociation pressure at ice point, atm
P_R	=	dissociation pressure of reference hydrate, atm
r	=	radial coordinate, $^{\circ}A$
R	=	gas constant, 1.987 cal/mole $^{\circ}K$; cell radius, $^{\circ}A$
T	=	temperature, $^{\circ}K$
T_o	=	temperature at ice point, 273.16 $^{\circ}K$
V	=	molar volume, cc/mole
V_W^α, V_W^β	=	molar volume of pure ice and empty hydrate lattice, respectively, cc/mole
$W(r)$	=	spherically -symmetric cell potential, ergs
X_W	=	mole fraction of liquid water
Y_ℓ	=	mole fraction of component ℓ in gas phase
Y_ℓ	=	mole fraction of component ℓ in hydrate phase

Greek Letters

Δ = indicates difference in thermodynamic property value of water in two phase

ε = depth of intermolecular potential well, erg

$\theta_{m\ell}$ = fraction of cavities type m occupied by component ℓ

μ = chemical potential, cal/mole

μ_W^H, μ_W^L, μ_W^α, μ_W^β = chemical potential of water in the hydrate phase, liquid phase, ice phase and empty hydrate, respectively, cal/mole

ν_m = number of cavities type m per water molecule in the hydrate

σ = the distance parameter when the Kihara potential is zero, ^OA

ϕ_ℓ = fugacity coefficient

Superscripts

0 = property at ice point

H = hydrate phase

L = liquid water phase

R = reference hydrate

α = ice phase

β = empty hydrate phase

Subscripts

j, ℓ	=	component
m	=	cavity type m
W	=	water

LITERATURE CITED

1. Villard, M., Compt. Rend., 106, 1602 (1888).

2. Ibid., 107, 395 (1888).

3. Villard, M., J. Phys., 5, 453 (1896).

4. Forcrand, M. R. de, Compt. Rend., 135, 959, (1902).

5. Hammerschmidt, E. G., Am. Gas Assoc. Monthly, 18, 278 (1936).

6. Hammerschmidt, E. G., Ind. Eng. Chem., 26, 851 (1934).

7. Hammerschmidt, E. G., Oil Gas J., 39, No. 2, 61 (1940).

8. Parent, J. D., Inst. Gas. Tech. Res. Bull. 1, (1948).

9. Barduhn. A. J., C. E. Prog. 63 (1), 98-103, (1967).

10. Barduhn, A. J., Towlson, H., and Yeechien Hu, A.I.Ch.E. Journ. 8 (2), 176-183 (1962).

11. Barrer, R. M. and Ruzicka, D. J., Trans. Fara. Soc. 58, 2239-2252.

12. Katz, D. L., J. Petr. Tech., 419-423 (1971).

13. Katz, D. L., J. Petr. Tech., 557-558 (1972).

14. Davidson, D. W. presented to the ACS meeting, Ottawa, June 9, 1980.

15. Parrish, William R. and John M. Prausnitz, Ind. Eng. Chem. Process Dev. Develop., Vol. 1. No. 4, 1972.

16. Faraday, M., Trans. Roy. Soc. (London), A22 (1823).

17. Deaton, W. M. and E. F. Frost, Jr., Proc. Am. Gas Assoc., pp. 168-203 (1940).

18. Hammerschmidt, E. G., I&EC., 26, 851-855 (1934).

19. Deaton, W. M. and Frost, E. M., "Gas hydrates and
     their relation to the operation of natural-gas
     pipelines," Monograph No. 8. U.S. Bureau of
     Mines (1946).

20. Deaton, W. M. and Frost, E. M., Am. Gas Assoc., Natural
     Gas Dept. Proc., 1937, 23, Am. Gas Assoc. Monthly,
     19, 219 (1937).

21. Kobayashi, R., Katz, D. L., Trans. A.I.M.E. (Tech.
     Note 294) 204, 262 (1955).

22. Scauzillo, F. R., Chem, Eng. Prog. 52 (8), 324 (1956).

23. Kolodeznii, P. A. and Arshinov, S. A., Russina J. Gas
     Bus. 11, (1970).

24. Katz, D. L., et al., "Handbook of Natural Gas Engine-
     ering," McGraw Hill Book Co., N. York.

25. Byk, S. Sh. and Fomina, V. I., Russ. Chem. Rev. 37 (6),
     469 (1978).

26. "Technical Data Book," Am. Petr. Inst., Petr. Refn.
     Dvn. Washington, D. C.

27. Stackelberg, M. Von, and Müller, H. R., F. Elektrochem.,
     58 (1), 40 (1954).

28. Pauling, L. and March, R. E., Proc. Nat. Acad. Sci.
     U.S.A., 38, 112 (1952).

29. Claussen, W. R., J. Chem. Phys. 19, 259 (1951).

30. Moeller, William, A. E. Higgins, George E. Welker,
     American Gas Assoc. Monthly, Mid-summer, 273,
     (1936).

31. Barrer, R. M. and Ruzicka, D. J., Trans. Fara. Soc.
     58, 2253 (1962).

32. Barrer, R. M. and Ruzicka, D. J., Trans. Fara. Soc.
     58, 2262 (1962).

33. Ceccotti, P. J., I. & E.C. Fundam., 5 (10), 106 (1966).

34. van der Waals, J. H. and Platteeuw, J. C., Advan. Chem. Phys., 2, 41 (1959).

35. von Stackelberg, M., Müller, H. R., Z. Elektrochem. 58, 25, (1954).

36. McKoy, V., Sinanoglu, O., J. Chem. Phys. 38, 2946 (1963).

37. Nagata, I., Kobayashi, R., Ind. Eng. Chem., Fundam. 5, 344 (1966).

38. Nagata, I., Kobayashi, R., Ind. Eng. Chem,. Fundam, 5, 466 (1966).

39. Emmerich, Wilhem, Rubin Battino, and Robert J. Wilcock, Chemical Reviews, Vol. 77, No. 2, 219-262 (1977).

40. Sloan, E. D. and Parrish, W. R., ACS Second Chemical Congress of the North American Continent, Las Vegas, August 25, (1980).

41. Holder, G. D., Corbin, G. and Papadopoulos, K. D., Ind. Eng. Chem. Fundam., 19, 282-286 (1980).

42. Wilcox, W. J., Carson, D. B, and Katz, D. L., I&EC, 33 (5), 662 (1941).

43. De Forcrand, R., Compt. Rend., 181, 15-17 (1925).

44. Godchot, Gauquil and Calas, Compt. Rend., 202, 759-760, 1936)

45. Miller, S. L., Private Communication, Nov. 6, 1980.

46. Ewing, Gordon J., and Ionescu, Lavinel G., Jour. of Chem. Eng. Data., 19 (4), 367-369 (1974).

47. Barrer, R. M., Edge, F.R.S. and A. V. J., Proc. Roy. Soc. (London), A300 (1460), 1-23 (1967).

48. Zerpa, Carlos, "An apparatus for the measurement of hydrate properties and the measurement of cyclo-propane solubility in Kcl solutions." Thesis No. 1975, Colorado School of Mines, 1977.

49. Menten, Paula Douglass, "The effect of the inhibitors
     potassium chloride, calcium chloride, and methanol
     on cyclopropane hydrate formation conditons."
     Thesis No. 2277, Colorado School of Mines, 1979.

50. Dharmawardhana, P. B., "The measurement of the thermo-
     dynamic parameters of the hydrate structure and the
     application of them in the prediction of the pro-
     perties of natural gas hydrates." Thesis No. 2218,
     Colorado School of Mines, 2980.

51. Tse, J. S. and Davidson, D. W., "Some Thermodynamic
     Aspects of Natural Gas Hydrates," 4th Canadian
     Permafrost Conference, Calgary, March 1981.

52. Hafemann, Dennis R. and Miller, Stanley L., "The Clath-
     rate Hydrates of Cyclopropane," Jour. of Phy. Chem.,
     73, 139201397 (1979).

53. Hafemann, Dennis R. and Miller, Stanley L., "The
     Duteric Hydrates of Cyclopropane," Jour. of Phy.
     Chem., 73, 1398-1401 (1969).

viii APPENDICES

A. Calibrations

1) Calibration of the Pressure Gauge

The pressure gauge was calibrated against a Ruska air dead weight tester. The range of pressure was from 15 to 84 psia. The results of the calibration are shown in Table A1. The procedure used to calibrate the pressure measuring system is outlined below.

Procedure: initially the pressure measuring system was connected to the calibration system. Plug in the dead weight tester after making sure the motor switch is in the "off" position. The necessary weights were removed using the test procedure in the manual, so that the piston does not jump up suddenly. At its mid position, switch the motor on and let the piston move freely. The temperature of the dead weight tester as well as the barometric pressure and the room temperature were recorded. Also, the dead weight number and the pressure gauge were recorded during the calibration.

where

m_a = $m_1 + m_2$

N_2 = weight of position

g_ℓ = local gravity

g_s = standard gravity

ρ_β = density of brass

ρ_{air} = density of air

A_o = area of the piston at zero psig and at the
         reference tem. 32^oC.

C = coefficient of supervicial expansion as
       indicated in the test report

B.P = barometric pressure in psia

ΔT = difference between working temperature and 23^oC

Table Al

Weight Number	P. Pressure of Gauge in psia	T °C
14	15.0	23.5
13	16.0	23.5
11	18.0	23.5
10	24.0	23.5
9	34.0	23.5
9 + 10	44.0	23.5
7	54.0	23.5
8	55.0	23.5
8 + 9	74.0	23.5
8 + 7	94.0	23.5
8 + 7 + 12	98.0	23.5
8 + 10	64.0	23.5
8 + 10 + 11	68.0	23.5
8 + 10 + 11 + 12	72.0	23.5
8 + 10 + 9	84.0	23.5

barometric pressure = 624.024 mm Hg = 12.069 psia. From
data table the pressure where calculated using the fol-
lowing equation

$$P_{cal} = ma \ (g_\ell/g_s) \ (\frac{\rho_\beta - \rho_{air}}{\rho_\beta})/A_o(1 + c \ \Delta T) + B.P$$

P of Heise Gauge, psia	P_{cal} psia	ΔP
15.0	15.06	0.06
16.0	16.06	0.06
18.0	18.06	0.06
24.0	24.05	0.05
34.0	34.04	0.04
44.0	44.03	0.03
54.0	54.02	0.02
74.0	73.99	-0.01
94.0	93.97	-0.03
98.0	97.97	-0.03
64.0	64.01	0.01
72.0	72.0	0.0
84.0	83.98	-0.02
68.0	68.006	0.006

2) Calibration of the Temperature Measurement

The temperature measurement system was calibrated against a Leeds and Northrup model 8.69 Muller bridge in conjunction with a Leeds and Northrup H-lead nominal 25 ohm platinum resistance thermometer. The Leeds and Northrup assembly was calibrated by the National Bureau of Standards to ± 0.0001°C.

Procedure: The Omega platinum resistance thermometer and the Leeds and Northrup platinum resistance thermometer were placed side by side in high quality cryostat bath which held a set point ± 0.005°C at all temperature within the experimental range. The data obtained was fit as a second order polynomical function of the Omega platinum resistance reading T_M (c).

$$T_{actual} = 0.3295 + 0.9982 \, T_{reading} + 0.002 \, T^2_{reading}$$

$T_{Northrup}$ platinum	T_{Omega} platinum	ΔT
-10.05	-10.4	0.35
0.11	- 0.2	0.09
5.21	4.8	0.41
9.83	10.2	0.37
15.04	14.7	0.34
20.04	19.6	0.44

B) <u>Data</u> <u>of</u> <u>Xenon</u> <u>Hydrate</u> <u>Below</u> <u>and</u> <u>Above</u> <u>273°K.</u>

  i) Data of xenon hydrate below 273°K

  1) Miller Data

  a) xenon hydrate Set I

$-T^{O}c$	$P_{xe}(mm)$
0.0	1130.3
2.51	1016.2
6.74	850.6
10.99	700.2
15.42	574.8
20.66	445.0
25.77	346.0
30.38	271.9
34.08	225.6
40.27	159.2
45.17	119.1
50.10	88.5
57.84	53.6
64.24	34.1
71.11	20.9
79.12	70.89
81.95	8.62
86.86	5.67

b)   Xenon Hydrate Set II

$-T\,^oC$	$P_{xe}(mm)$
0.0	1130.3
2.27	1032.0
6.38	862.1
11.23	694.9
15.39	581.5
20.00	457.2
23.75	379.6
25.06	346.2
28.50	298.7
30.26	272.2
35.48	205.7
37.09	189.2
45.86	113.4
55.82	60.8
66.63	28.7

2) Barrer and Edge Data

Temp (^{O}K)	Decomposition Pressure (cm Hg)
268.2	9.10
153.3	48.6
238.2	23.1
239.4	14.53
223.0	10.16
211.2	4.90

ii) Data of Xenon Hydrate Above 273°K

a) Present Work

T^{O}F	P_{xe} (psia)
32.0	22.1
33.6	24.0
34.7	25.6
36.5	28.8
37.9	31.2
39.4	34.3
41.0	37.8
41.9	39.6
43.2	42.6
44.1	45.0
45.3	48.5
46.6	52.2

a)   Present Work (cont.)

$T^{o}F$	$P_{xe}(psia)$
47.5	55.0
48.6	58.7
50.0	63.7

b)   Data of Forcrand

$T^{o}F$	$P_{xe}(psia)$
34.52	21.31
41.0	31.97
46.4	43.91
50.0	55.27

c)   Data of Godchot

$T^{o}F$	$P_{xe}(psia)$
35.6	25.28
39.2	31.02
42.8	37.92
46.4	47.77
50.0	59.83

d) Data by Ewing & Ionescu

$T\,^oF$	$P_{xe}(psia)$
32.0	22.34
35.6	25.97
39.2	31.99
41.0	36.55
42.8	41.14
46.4	49.71
50.0	60.73

e) Data by Bernhard Braun

$T\,^oF$	$P_{xe}(psia)$
32.0	22.12
35.6	27.78
39.2	34.69
42.8	42.77
46.4	53.21
50.0	66.44

f) Data by Louwrens Aaldijk

T^oC	P_{xe} atm
0.0	1.504
0.34	1.568
0.41	1.571
0.67	1.613
1.28	1.717
1.60	1.771
1.68	1.787
2.59	1.946
3.52	2.144
4.51	2.368
5.52	2.641
6.41	2.905
7.47	3.231
8.51	3.583
9.51	3.977
10.47	4.394
11.51	4.865
12.51	5.439
9.03	3.82
10.13	4.27
10.90	4.60
12.02	5.17

C) Sample of Calculation

Estimation of Hydrate numbers

From the P-T data below and above $0^{\circ}C$ the heat of formation was calculated according to the following equation:

$$\ln P = A + \frac{B}{T}$$

Now by differentiating the above equation we get

$$\frac{d \ln P}{d \left(\frac{1}{T}\right)} = B$$

From the Clausius relation

$$\frac{d \ln P}{d \left(\frac{1}{T}\right)} = \frac{\Delta H}{R}$$

Thus

$$-\frac{\Delta H}{R} = B$$

Now the P-T data was fit with a stepwise multiple linear regression program the following values of A and B are obtained:

Range of temperature	A	B	No. of Data Points
0 to - 86.8	14.566875	-3134.00	18
0 to $10^{\circ}C$	34.767	08130.72	15

Calculation of ΔH below and above $0^{\circ}C$

From the above table $B = -3134.00$

$\Delta H_1 = -R \times B = 1.987 \times 3134.00 = 6227.259$ cal/gmol

$\Delta H_2 = -R \times B = 1.987 \times 8130.72 = 16155.74$ cal/gmol

Calculation of n

$$n = \frac{\Delta H_2 0 - \Delta H_1}{\Delta H_f}$$

$\Delta H_f = 1437.00$ cal/gmol

$$n = \frac{16155.74 - 6227.258}{1437.00} = 6.91 \ \frac{\text{gmoles } H_2 0}{\text{gmoles } X_e}$$

Calculation of Y gmoles of X_e/gmoles H_2O

By using the following equation

$Y_A = \frac{1}{n}$ where Y_A is total moles of A in clathrate/mole H_2O

We get

$$Y_A = \frac{1}{6.91} = 0.1447 \ \text{gmoles } X_e/\text{gmoles } H_2 0$$

Calculation of θ_L and θ_S

From van der Walls and Platteeuw we have the follow-ing equation:

$$Y_A = \Sigma_i \ v_i \ \theta_{Ai}$$

$$Y_A = V_s \ \theta_{AS} + V_L \ \theta_{AL}$$

From Davidson (1980) NMR we know that the ratio between $\theta_{AL}/\theta_{AS} = 1.30$

Thus

$$\theta_{AL} = 1.30 \ \theta_{AS}$$

Now

$$Y_A = \frac{1}{23} \ \theta_{AS} + \frac{3}{23} \ \theta_{AL}$$

$$= \frac{1}{23} \ \theta_{AS} + \frac{3}{23} (1.30 \ \theta_{AS})$$

$$= 0.2121 \ \theta_{AS}$$

Since Y_A is known then one can get θ_{AS}

$$0.1447 = 0.2121 \ \theta_{AS}$$

$$\theta_{AS} = \frac{0.1447}{0.2121} = 0.6791$$

$$\theta_{AL} = 1.30 \ \theta_{AS} = 0.8829$$

Calculation experimental Langmuir constants

Langmuir equation is given as follows:

$$\theta_{Ai} = C_{Ai} \ fA/1 + C_{Ai} \ f_A$$

Where A is the molecule type

i is the cavity type L or S

for X_e at $0^{\circ}C$ we take $f_A = 1.472$ ATM

<u>for</u> <u>small</u> <u>cavities</u>

$$0.6791 = \frac{1.472\ C_{AS}}{1 + 1.472\ C_{AS}}$$

solving for C_{AS} we get $C_{AS} = 1.4377$

<u>for</u> <u>large</u> <u>cavities</u>

$$0.8829 = \frac{1.472\ C_{AL}}{1 + 1.472\ C_{AL}}$$

solving for C_{AL} we get

$$C_{AL} = 5.1212$$

<u>Calculation of chemical potential difference</u> $\underline{\Delta\mu_{0,0}}$ <u>cal/gmol</u>

We know that the chemical potential difference is given
by the following equation:

$$\Delta\mu\ (T,P) = RT\ \Sigma\ v_i\ \ln\ (1 + C_A\ fi)$$

$$= RT\left\{\frac{1}{23}\ \ln\ (1 + C_{AS}\ fi) + \frac{3}{23}\ \ln\ (1 + C_{AL}\ fi)\right\}$$

$$= 1.987\cdot(273.0)\left\{\frac{1}{23}\ \ln\ (1 + 1.4377 \times 1.472)\right.$$

$$\left. + \frac{3}{23}\ \ln\ (1 + 5.1212 \times 1.472)\right\}$$

$$= 542.45/0\left\{\ 0.0494 + 0.2797\ \right\}$$

$$= 178.53\ cal/gmol$$

D) Computer Programs

i) Computer Program HYDXEN.FOR

The compute program HYDXEN.FOR calculates forma-
tion conditions in moist gas mixtures. The method of solu-
tion uses the statistical thermodynamic theory. The program
is written in FORTRAN IV. It is easy to use.

The Kihara parameters, the numbers to identify
the cavities of Structures I and II that could be filled
by the guest molecules, solubility data and the critical
properties of the component are to be supplied to the main
program through the data file FOR15.DAT in the following
sequence:

1st line = The Kihara paramters

ε/K, σ , a

2nd line = Identification numbers to indicate
the possibility of filling of the hydrate cavities of Struc-
tures I and I. Arbitary numbers 20 and 0.0 were used to
indicate filled and empty cavities. The data sequence is
illustrated below:

small cavity, large cavity, small cavity, large cavity
Structure I   Structure I   Structure II Structure II

3rd line = The solubility data to calculate the
solubility of component in liquid water. The solubility
was calculated by the equation:

R ln (mole fraction of = A + B/T + C ln T + DT

Component i in water)

Where A, B, C and D are constants. The numerical values for the constants A, B, C and D for xenon was taken from the work of E. Wilhelm et al., (36). The data sequence is A, B, C, D.

4th line = The critical properties. The data sequence are given below:

critical, critical, critical, acentric

temp.   pressure   volume   factor

The equilibrium data have to be supplied to the computer program through the data file FoR92.DAT in the following sequence:

Temp. (^{O}F), first guess for,   Vapor phase of mole

pressure (Exp. psia)   fraction of components

Hydrate structure and the number of data points have to be supplied to the program at execution according to the FORMAT (30G).

ii) Computer Program HYD.FOR

The program HYD.FOR reduces hydrate dissociation pressure-temperature data to obtain Kihara (spherical-core) parameters using the program CNEW.FOR for optimization.

The program is written in FORTRAN.IV. The critical properties of the component, the solubility data and the

equilibrium data have to be supplied to the computer pro-

gram through the data file FoRo7.DAT in the following

sequence

1st line = The critical properties. The data

sequence are critical temp.; critical pressure, critical

volume, acentric factor.

2nd line = The solubility data to calculate the

solubility of xenon in liquid water. The solubility was

calculated by the equation:

R ln (mole fraction of xenon in water)

$$= A + \frac{B}{T} + C \ln T + DT$$

The numerical values of constants A, B, C, and D was taken

from the (36). The data sequence is A, B, C, D.

3rd line = The equilibrium data (i.e. the experimental

data) in the following sequence.

Temperature (^{O}F), Pressure (psia)

Hydrate structure and the number of data points have

to be supplied to the program at execution according to the

FORMAT LOG

```
C     ----------------------------------------------------------------
C                     COMPUTER PROGRAM HYD.FOR
C     ----------------------------------------------------------------
C     THE COMPUTER PROGRAM HYD.FOR REDUCES HYDRATE DISSOCIOTION
C     PRESSUR-TEMPERATURE DATA TO OBTAIN KIHARA(SPHERICAL-CORE)
C     PARAMETERS USING THE COMPUTER PROGRAM CENW.FOR .
C     ----------------------------------------------------------------
      DIMENSION TC(10),PC(10),W(10),B(10),PHI(10),VC(10),AK(10)
     1,A(100,100),Y(10),TR(10),PR(10),CG(100,100)
      DIMENSION SO1(10),SO2(10),SO3(10),SO4(10)
      NCOMP=1
      READ(07,10)TC(1),PC(1),VC(1),W(1)
      READ(07,10)SO1(1),SO2(1),SO3(1),SO4(1)
      READ(4,10)NHY,NPT
      DO 279 INPT=1,NPT
      READ(07,10)T,P
      Y(1)=1.
      TT=T
      PP=P
      T=(T-32.)*5./9.+273.16
      P=P/14.696
C     CALL ACT(SO1,SO2,SO3,SO4,T,ACTI,NCOMP)
      R=82.056
      ID=-1
      DO 97 I=1,NCOMP
      DO 97       J=1,NCOMP
      A(I,J)=.0
      AM=.0
      BM=.0
      B(I)=.0
      AK(I)=.0
97    CONTINUE
10    FORMAT(10G)
      DO 1 I=1,NCOMP
      TR(I)=T/TC(I)
      IF(Y(I).EQ..0) GO TO 149
      PR(I)=P/PC(I)
      A(I,I)=.45724*(R*TC(I))**2/PC(I)
      B(I)=.0778*R*TC(I)/PC(I)
103   FORMAT(1X,'I,A(II)',I2,X,F15.3)
      AK(I)=.37464+1.54226*W(I)-.26992*W(I)**2
102   FORMAT(1X,'I,K',I2,X,F10.5)
      AK(I)=(1.+AK(I)*(1.-SQRT(TR(I))))**2
      A(I,I)=AK(I)*A(I,I)
30    FORMAT(1X,'TR,PR,A(I,I),B',5F13.4,X)
149   CONTINUE
1     CONTINUE
      DO 2 I=1,NCOMP
      DO 2 J=1,NCOMP
      IF(Y(J).EQ..0) GO TO 145
      IF(Y(I).EQ..0) GO TO 145
```

```
            A(I,J)=(1.-CG(I,J))*SQRT(A(I,I)*A(J,J))
81          FORMAT(1X,2(I2,X),F15.5)
145         CONTINUE
2           CONTINUE
            DO 4 I=1,NCOMP
            IF(Y(I).LE..0) GO TO 41
41          CONTINUE
            BM=BM+B(I)*Y(I)
4           CONTINUE
            DO 75      I=1,NCOMP
            AK(I)=.0
75          CONTINUE
            DO 3 J=1,NCOMP
            DO 3 I=1,NCOMP
            IF(Y(I).EQ..0) GO TO 148
            IF(Y(J).EQ..0) GO TO 148
            AK(J)=Y(I)*A(I,J)+AK(J)
148         CONTINUE
3           CONTINUE
            DO 6 J=1,NCOMP
            AK(J)=2.*AK(J)
85          FORMAT(1X,F15.4)
6           CONTINUE
              DO 5 I=1,NCOMP
              DO 5 J=1,NCOMP
            AM=AM+Y(I)*Y(J)*A(I,J)
5           CONTINUE
40          FORMAT(1X,2F15.5,X)
            CALL VCUBE(AM,BM,P,R,T,V,Z,ID)
83          FORMAT(1X,'Z',F10.5)
            AB=AM*P/(R*T)**2
            BB=BM*P/(R*T)
            DO 62      I=1,NCOMP
            IF(Y(I).EQ..0) GO TO 61
            A1=B(I)*(Z-1.)/BM
            A2=ALOG(Z-BB)
            A3=AB/(2*SQRT(2.)*BB)
86          FORMAT(1X,4(F15.3,X))
            A4=AK(I)/AM-B(I)/BM
            A5=ALOG((Z+2.414*BB)/(Z-.414*BB))
84          FORMAT(1X,4(F10.4,X))
            PHI(I)=A1-A2-A3*A4*A5
            PHI(I)=EXP(PHI(I))
            PHI(I)=PHI(I)*Y(I)*P
61          CONTINUE
62          CONTINUE
            CALL AMU(T,P,SO1,SO2,SO3,SO4,DMU2,NHY,NCOMP)
C           ACTI=0.0
            WRITE(10,300)TT,PP,PHI(1),PHI(2),DMU2,ACTI
300         FORMAT(1X,6(F10.3,X))
279         CONTINUE
```

```
            STOP
            END
```

```
      SUBROUTINE VCUBE(A,B,P,R,T,V,Z,ID)
      D=B-R*T/P
      E=-(3.*B*B+2.*R*T*B/P-A/P)
      F=B*B*B+(R*T*B*B-A*B)/P
        G=(3.*E-D*D)/3.
        H=-(9.*D*E-27.*F-2.*D*D*D)/27.
        IF(G**3./27.+H*H/4..LE.0.) GO TO 10
        S=-H/2.+SQRT(G**3./27.+H*H/4.)
        TT=-H/2.-SQRT(G**3./27.+H*H/4.)
        IF(S)5,6,6
5       S=-((-S)**(1./3.))
        GO TO 7
6       S=(S)**(1./3.)
7       IF(TT)8,9,9
8       TT=-(-TT)**(1./3.)
        GO TO 15
9       TT=(TT)**(1./3.)
C     SINGLE REAL ROOT
15      V=S+TT-D/3.
        GO TO 40
10      THETA = (ACOS(-.5*H/SQRT(-G**3/27.)))/3.
        V1=2.*SQRT(-G/3.)*COS(THETA)
        V2=2.*SQRT(-G/3.)*COS(THETA+2.0944)
        V3=2.*SQRT(-G/3.)*COS(THETA+4.1888)
        IF(ID)20,30,30
C     TAKE LARGEST V FOR VAPOR
20      V=AMAX1(V1,V2,V3)-D/3.
        GO TO 40
C       TAKE SMALLEST V FOR LIQUID
30    V=AMIN1(V1,V2,V3)-D/3.
40    Z=P*V/(R*T)
      RETURN
      END
```

```
      SUBROUTINE AMU(T,P,S01,S02,S03,S04,DMU2,NHY,NCOMP)
      DIMENSION S01(10),S02(10),S03(10),S04(10),X(10)
      IF(T.LT.237.16) ACTI=0.0
      NCOMP=1
      DO 1 I=1,NCOMP
      X(I)=S01(I)+S02(I)/T+S03(I)*ALOG(T)+S04(I)*T
      X(I)=EXP(X(I)/1.987)
      XW=1.-X(I)
1     CONTINUE
      ACTI=1.987*T*ALOG(XW)
      IF(NHY.GT.1) GO TO 20
C     CALCULATE STRUCTURE I PROPERTIES
      V=6./46.
C     CALCULATE STRUCTURE II PROPERTIES
20    V=8./136.
      IF(NHY.GT.1) GO TO 60
C     CALCULATE STRUCTURE I PROPERTIES
      DV=4.598
      IF(NHY.EQ.1) GO TO 233
233   DH=332.0
      DM=310.
      IF(T.GT.273.16) GO TO 70
      DV=3.
      GO TO 70
C     CALCULATE STRUCTURE II PROPERTIES
60    DV=4.998
      DH=245.
      DM=224.
      IF(T.GT.273.) GO TO 70
      DV=3.4
70    TO=273.16
C     CALCULATE ENTHALPY INTEGRAL
      HINT=(1./1.987)*(DH*(1./T-1./TO)+2616.398*(1./T-
     11./TO)+20.6166*ALOG(T/TO)-0.021163*(T-TO))
      IF(T.LT.273.16) HINT=(1./1.987)*(DH*(1./T-1./TO)
     1-19.053*(1./T-1./TO)-4.464E-3*ALOG(T/TO)+2.390E-4*(T-TO))
115   FORMAT(1X,2F15.5)
      IF(NHY.EQ.1)  DV=4.598
      DMU2=(DM/(1.987*273.16)+HINT)*(1.987*T)-ACTI+DV*0.024152*P
112   FORMAT(1X,3(F10.4,X))
      RETURN
      END
```

```
        SUBROUTINE ACT(SO1,SO2,SO3,SO4,T,ACTI,NCOMP)
        DIMENSION SO1(10),SO2(10),SO3(10),SO4(10),X(10)
C       IF(T.LT.273.16) GO TO 200
        DO 1 I=1,NCOMP
        X(I)=SO1(I)+SO2(I)/T+SO3(I)*ALOG(T)+SO4(I)*T
        X(I)=EXP(X(I)/1.987)
        XSUM=XSUM+X(I)
1       CONTINUE
        XW=1.-XSUM
        ACTI=1.987*T*ALOG(XW)
        XSUM=.0
200     IF(T.LT.273.16) ACTI=.0
        RETURN
        END
```

```
       DIMENSION CL(4,10),EP(10),SIGP(10)
      1, PHI(50,50),AM(50),TX(50)
      2,CB(4,10),CP(10)
       READ(08,10)CB(1,1),CB(2,1),CB(3,1),CB(4,1),CP(1)

       N=0
       READ(04,10)EP(1),SIGP(1),NHY
       READ(04,10)NT,DEP,DSIGP
       READ(04,10)NRUN,NNX
       XINC=-NNX*DSIGP
12     REWIND 10
       TDEVI=.0
       DEVI=.0
       DO 1 II=1,NT
       READ(10,10)T,P,PHI(1,1),PHI(2,2),DMU2,AC
       T=(T-32.)*5./9.+273.15
       TT=T
       P=P/14.696
       PP=P
       CALL LANG(T,CL,EP,SIGP,CB,CP)
       IF(NHY.GT.1) GO TO 3
       AM1=2.*ALOG(1.+CL(1,1)*PHI(1,1))/46.
       AM2=6.*ALOG(1.+CL(2,1)*PHI(1,1))/46.
       GO TO 4
3      AM1=16.*ALOG(1.+CL(3,1)*PHI(1,1))/136.
       AM2=8.*ALOG(1.+CL(4,1)*PHI(1,1))/136.
4      AMUCAL=(AM1+AM2)*1.987*TT+AC
       DEVI=ABS(AMUCAL-DMU2)
       TDEVI=DEVI+TDEVI
1      CONTINUE
       DEVIM=TDEVI/NT
110    FORMAT(1X,'TTT',3(F15.5,X))
       N=N+1
               IF(N.GT.1) GO TO 90
       DSAVE=DEVIM
       SIGP(1)=SIGP(1)+DSIGP
       GO TO 12
90     DIF=(DEVIM-DSAVE)/DSIGP
       DSAVE=DEVIM
               IF(DIF) 40,70,60
40     NNX=NNX-1
       IF(NNX.EQ.0) GO TO 70
       NNX=-1
       GO TO 100
60     NNX=NNX+1
       IF(NNX.EQ.0) GO TO 70
       NNX=1
       GO TO 100
70     WRITE(4,202)DEVIM,EP(1),SIGP(1)
       WRITE(01,20)DEVIM,EP(1),SIGP(1),CP(1)
       NIT=NIT+1
```

```
        IF(NIT.GT.NRUN) STOP
        SIGP(1)=SIGP(1)+XINC
        N=0
        EP(1)=EP(1)-DEP
        GO TO 12
100     SIGP(1)=SIGP(1)+DSIGP
        GO TO 12
        STOP
10      FORMAT(10G)
20      FORMAT(1X,3(F11.5,2X),F12.8)
202     FORMAT(1X,3(F15.5,X))
        END
```

```
      SUBROUTINE LANG(T,CL,EP,SIGP,CB,CP)
      DIMENSION A(4),Z(4),CB(4,10),KS(10),CL(4,10),
     1X(20),WT(20),SIGP(10),EP(10),CP(10)
      NPT=10
      NP=5
      DATA(X(J),WT(J),J=6,10)/.1488743389,.29552422147,
     1.4333953941,.2692667193,.6794095683,.2190
     22863625,.86506336627,.1494513492,.9739065285,
     33.0666713443/
      DATA (A(I),Z(I),I=1,4)/3.95,20.,4.3,24.,3.91,20.,4.73,
     1128./
      DATA PI,BK/3.1416,1.3804E-16/
      DO 22 J=1,NP
      X(J)=-X(NPT-J+1)
      WT(J)=WT(NPT-J+1)
22    CONTINUE

      KBLOW=0
      DO 5 J=1,1
      DO 1 I=1,4
1     CL(I,J)=.0
      C=CP(J)
      EK=EP(J)
      EC=EP(J)*BK
      RC=SIGP(J)*1.122462
      DO 5 I=1,4
      IF (CB(I,J).LT.1.) GO TO 5
      RCA=RC/A(I)
            CA=C/A(I)
C     NEWTON RAPSON METHOD FOR FINDING LIMITS , YL
C     FIRST GUESS S=.4
      S=.4
      RCA6=RCA**6
      RCA12=RCA**12
      DO 2 N=1,20
      IF (S.GT.1.0.OR.S.LE.0.0) GO TO 6
      UM=1./(1.-S-CA)
      UP=1./(1.+S-CA)
      UM5=UM**5
      UP5=UP**5
      DA4=UM5+UP5
      DA5=UM5*UM+UP5*UP
      DB6=DA4+CA*DA5
      UM11=UM**11
      UP11=UP**11
      DA10=UM11+UP11
      DA11=UM11*UM+UP11*UP
      DB12=DA10+CA*DA11
      DB=RCA12*DB12-2.*RCA6*DB6
      A10=UM11/UM-UP11/UP
      A11=UM11-UP11
```

```
                B12=(.1*A10+CA*A11/11.0)
                A4=UM5/UM-UP5/UP
                A5=UM5-UP5
                B6=A4/4.+CA*A5/5.
                B=RCA12*B12-2.*RCA6*B6
                W=Z(I)*EK/(2.*S*T)*B
                DWY=-W/S+Z(I)*EK*DB/(2.*S*T)
                DS=S-(W-10.)/DWY
                IF(ABS((DS-S)/DS).LT.0.01) GO TO 3
     2          S=DS
     3          YL=S
     C          GAUSSIAN INTEGRATION
                P=2.*PI*A(I)**3/(T*136.2)*YL
                SQ=.0
                DO 4 N=1,NPT
                Y=YL*(X(N)+1.)/2.
                UP=1./(1.+Y-CA)
                UM=1./(1.-Y-CA)
                UP5=UP**5
                UM5=UM**5
                A4=UM5/UM-UP5/UP
                A5=UM5-UP5
                B6=A4/4.+CA*A5/5.
                UP11=UP**11
                UM11=UM**11
                A10=UM11/UM-UP11/UP
                A11=UM11-UP11
                B12=(.1*A10+CA*A11/11.)
                B=RCA12*B12-2.*RCA6*B6
                W=Z(I)*EK/(2.*Y*T)*B
     4          SQ=SQ+EXP(-W)*Y**2*WT(N)
                CL(I,J)=P*SQ
     5          CONTINUE
                RETURN
     6          KBLOW=2
                WRITE(4,7)
     7          FORMAT(1X,'PROBLEM BLOW UP')
                RETURN
                END
```

```
C          ----------------------------------------------------------
C                        COMPUTER PROGRAM HYDXEN.FOR
C          ----------------------------------------------------------
C          THE COMPUTER PROGRAM HYDXEN.FOR CALCULATE HYDRATE-FORMATION
C          CONDITIONS.THE METHOD OF SOLUTION USES STATISTICL THERMODNAMIC
C          THEORY OF VAN DER WAALS AND PLATTEEUW.
C          ----------------------------------------------------------
           DIMENSION CL(4,10),PHI(10),Y(10),DMU(2)
           DIMENSION EP(10),SIGP(10),CP(10),CB(4,10),SO1(10)
          1,SO2(10),SO3(10),SO4(10),TC(10),PC(10),VC(10),W(10)
           DIMENSION D(2),VU(2),VL(2)
140        FORMAT(1X,4(F10.5,X))
           READ(4,10)NHY,NN
           NCOMP=1
           PINCX=.001
           DO 21 I=1,NCOMP
           READ(15,10) EP(I),SIGP(I),CP(I)
304        FORMAT(1X,4(F10.5,X))
21         CONTINUE
           DO 3 I=1,NCOMP
           READ(15,10)CB(1,I),CB(2,I),CB(3,I),CB(4,I)
3          CONTINUE
           DO 4 I=1,NCOMP
           READ(15,10) SO1(I),SO2(I),SO3(I),SO4(I)
4          CONTINUE
           DO 6         I=1,NCOMP
           READ(15,10)TC(I),PC(I),VC(I),W(I)
6          CONTINUE

           DO 1 IX=1,NN
           READ(02,10)T,P,Y(1)
           DS=.0
           NG=NG+1
           NSF=0
           NR=0
           NEWPT=0
           PEX=P
           P=P/14.696
           T=(T-32.)*5./9.+273.15
530        CONTINUE
           CALL LANG(T,CL,EP,SIGP,CP,NCOMP,CB)
25         FORMAT(1X,2(F10.5,X))
           CL(4,4)=4.040815/T*EXP(2687.9744/T)
           CL(4,5)=7.046619/T*EXP(3083.9044/T)
           CALL ACT(SO1,SO2,SO3,SO4,T,ACTI,NCOMP,Y)
111        CONTINUE
           DO 660 K=1,2
900        FORMAT(1X,5(F10.4,X))
112        CALL PENG(T,P,NCOMP,Y,PHI,TC,PC,VC,W)
           CALL AMUC(T,P,NHY,AMU)
10         FORMAT(30G)
```

```
           IF(NHY.GT.1) GO TO 18
           DO 17 I=1,NCOMP
           IF(Y(I).EQ..0) GO TO 610
           CSML=CL(1,I)*PHI(I)
           CSMLS=CSMLS+CSML
           CLG=CL(2,I)*PHI(I)
           CLGS=CLG+CLGS
      610  CONTINUE
      17   CONTINUE
           AM1=2.*ALOG(1.+CSMLS)/46.
           AM2=6.*ALOG(1.+CLGS)/46.
           DMCAL=(AM1+AM2)*1.987*T
           CSMLS=.0
           CLGS=.0
           GO TO 20
      18   DO 19 I=1,NCOMP
           IF(Y(I).EQ..0) GO TO 620
           CSML=CL(3,I)*PHI(I)
           CSMLS=CSMLS+CSML
           CLG=CL(4,I)*PHI(I)
           CLGS=CLG+CLGS
      620  CONTINUE
      19   CONTINUE
           AM1=16.*ALOG(1.+CSMLS)/136.
           AM2=8.*ALOG(1.+CLGS)/136.
           DMCAL=(AM1+AM2)*1.987*T
           CSMLS=.0
           CLGS=.0
      20   DEL=AMU-DMCAL
           WRITE(03,711)P,DEL
      711  FORMAT(1X,2(F10.4,X))
           WRITE(20,701)P,DEL,DPS,DS,AMU,NG,NR
      701  FORMAT(1X,'P,DEL,DPS,DS,AMU,NORD,NSF',5(F10.3,X),2(I3,X))
           IF(NR.EQ.1) GO TO 702
      694  CONTINUE
           D(K)=DEL
      662  DPS=ABS(DEL)*100./AMU
           IF(DPS.LT..1) GO TO 80
           P=P+PINCX
      660  CONTINUE
           DPS=(DEL/AMU*100)
           IF(ABS(DPS).LT..1) GO TO 80
           NEWPT=NEWPT+1
           IF(NEWPT.EQ.1) GO TO 800
           NTEST=DS/ABS(DS)+DEL/ABS(DEL)
           IF(NTEST.EQ.0) GO TO 702
           IF(ABS(DEL).GT.ABS(DS)) GO TO 703
      800  PS=P
           DS=DEL
           P=P-DEL/((D(2)-D(1))/PINCX)
           K=0
```

```
        GO TO 111
80      T=(T-273.15)*9./5.+32.
        P=P*14.696
        DPSUM=DPSUM+ABS(PEX-P)
        WRITE(4,43)Y(1),T,PEX,P
7       K=0
        N=0
        NR=0
        NC1=0
        NU1=0
        NUM=0
  NU=0
        NRC=0
43      FORMAT(1X,(F8.3,X),3(F7.1,X))
1       CONTINUE
        PDMN=DPSUM/NN
        WRITE(10,34)PDMN
34      FORMAT(1X,F10.2)
        STOP

702     CONTINUE
        DEL=AMU-DMCAL
        DPS=ABS(DEL)*100./AMU
        IF(NR.EQ.1) GO TO 51
51      IF(DPS.LT..1) GO TO 80
        DSAVE=DEL
52      FORMAT(1X,2(F10.3,X))
        NR=1
        NRC=1+NRC
        IF(NRC.GT.1) GO TO 668
        U1=DEL
        U2=DS
        U3=P
        U4=PS
44      FORMAT(1X,4(F10.5,X))
        GO TO 690
668     U2=DEL
        U4=P
        NUM=DEL/ABS(DEL)
        IF(NUM)670,672,676
670     U1=AMAX1(VU(1),VU(2))
        GO TO 675
676     U1=AMIN1(VU(1),VU(2))
        GO TO 675
672     WRITE(4,681)
681     FORMAT(1X,'CHECK CONVERGENCE')
        STOP
675     CONTINUE
        DO 682 II=1,2
        IF(U1.EQ.VU(II)) U3=VL(II)
682     CONTINUE
```

```
690     P=(U1*U4-U2*U3)/(U1-U2)
        VU(1)=U1
        VU(2)=U2
        VL(1)=U3
        VL(2)=U4
49      FORMAT(1X,'VU &VL',4(F10.4,X))
        GO TO 111
703     T=(T-273.15)*9./5.+32.
        P=PS*14.696
        WRITE(10,704)T,PEX,P
704     FORMAT(23X,'*',3(F10.3),X)
        GO TO 7
        STOP
        END
```

```
      SUBROUTINE AMUC(T,P,NHY,DMU2)
10    FORMAT(3F)
      IF(NHY.GT.1) GO TO 20
C     CALCULATE STRUCTURE I PROPERTIES
      V=6./46.
C     CALCULATE STRUCTURE II PROPERTIES
20    V=8./136.
C     CALCULATE LN OF ACTIVITY
C     CALCULATE STRUCTURE I PROPERTIES
      DV=4.598
      DH=402.
      DM=310.0
      GO TO 70
C     CALCULATE STRUCTURE II PROPERTIES
      DV=4.998
      DH=245.
      DM=224.
70    TO=273.15
C     CALCULATE MUO/RTO AT PO,TO
C     CALCULATE ENTHALPY INTEGRAL
      HINT=(1./1.987)*(DH*(1./T-1./TO)+2616.398*(1./T-
     11./TO)+20.6166*ALOG(T/TO)-.021163*(T-TO))
      IF(T.LT.273.16) HINT=(1./1.987)*(DH*(1./T-1./TO)
     1-19.053*(1./T-1./TO)-4.464E-3*ALOG(T/TO)+2.390E-4*(T-TO))
      IF(NHY.EQ.1) DV=4.598
      CALL ACT(SO1,SO2,SO3,SO4,T,ACTI,NCOMP,Y)
      DMU2=(DM/(1.987*273.16)+HINT)*(1.987*T)-ACTI+DV*0.0242152*P
115   FORMAT(1X,F15.2)
      RETURN
      END
```

```
            SUBROUTINE LANG(T,CL,EP,SIGP,CP,NCOMP,CB)
            DIMENSION A(4),Z(4),CB(4,10),KS(10),CL(4,10),
           1X(20),WT(20),SIGP(10),EP(10),CP(10)

            NPT=10
            NP=5
            DATA(X(J),WT(J),J=6,10)/.1488743389,.29552422147,
           1.4333953941,.2692667193,.6794095683,.2190
            2863625,.86506336627,.1494513492,.9739065285,
            3.0666713443/
            DATA (A(I),Z(I),I=1,4)/3.95,20.,4.3,24.,3.91,20.,4.73,
           128./
            DATA PI,BK/3.1416,1.3804E-16/
            DO 22 J=1,NP
            X(J)=-X(NPT-J+1)
            WT(J)=WT(NPT-J+1)
22          CONTINUE

            KBLOW=0
            DO 5 J=1,NCOMP
            DO 1 I=1,4
1           CL(I,J)=.0
            C=CP(J)
            EK=EP(J)
            EC=EP(J)*BK
            RC=SIGP(J)*1.122462
            DO 5 I=1,4
            IF (CB(I,J).LT.1.) GO TO 5
            RCA=RC/A(I)
            CA=C/A(I)
C           NEWTON RAPSON METHOD FOR FINDING LIMITS , YL
C           FIRST GUESS S=.4
            S=.4
            RCA6=RCA**6
            RCA12=RCA**12
            DO 2 N=1,20
            IF (S.GT.1.0.OR.S.LE.0.0) GO TO 6
            UM=1./(1.-S-CA)
            UP=1./(1.+S-CA)
            UM5=UM**5
            UP5=UP**5
            DA4=UM5+UP5
            DA5=UM5*UM+UP5*UP
            DB6=DA4+CA*DA5
            UM11=UM**11
            UP11=UP**11
            DA10=UM11+UP11
            DA11=UM11*UM+UP11*UP
            DB12=DA10+CA*DA11
            DB=RCA12*DB12-2.*RCA6*DB6
            A10=UM11/UM-UP11/UP
```

```
            A11=UM11-UP11
            B12=(.1*A10+CA*A11/11.0)
            A4=UM5/UM-UP5/UP
            A5=UM5-UP5
            B6=A4/4.+CA*A5/5.
            B=RCA12*B12-2.*RCA6*B6
            W=Z(I)*EK/(2.*S*T)*B
            DWY=-W/S+Z(I)*EK*DB/(2.*S*T)
            DS=S-(W-10.)/DWY
            IF(ABS((DS-S)/DS).LT.0.01) GO TO 3
      2     S=DS
      3     YL=S
      C     GAUSSIAN INTEGRATION
            P=2.*PI*A(I)**3/(T*136.2)*YL
            SQ=.0
            DO 4 N=1,NPT
            Y=YL*(X(N)+1.)/2.
            UP=1./(1.+Y-CA)
            UM=1./(1.-Y-CA)
            UP5=UP**5
            UM5=UM**5
            A4=UM5/UM-UP5/UP
            A5=UM5-UP5
            B6=A4/4.+CA*A5/5.
            UP11=UP**11
            UM11=UM**11
            A10=UM11/UM-UP11/UP
            A11=UM11-UP11
            B12=(.1*A10+CA*A11/11.)
            B=RCA12*B12-2.*RCA6*B6
            W=Z(I)*EK/(2.*Y*T)*B
      4     SQ=SQ+EXP(-W)*Y**2*WT(N)
            CL(I,J)=P*SQ
      270   FORMAT(1X,4(F10.5,X))
      5     CONTINUE
            RETURN
      6     KBLOW=2
            WRITE(4,7)
      7     FORMAT(1X,'PROBLEM BLOW UP')
            RETURN
            END
```

```
      SUBROUTINE PENG(T,P,NCOMP,Y,PHI,TC,PC,VC,W)
      DIMENSION TC(10),PC(10),W(10),B(10),PHI(10),VC(10),AK(10)
     1,A(100,100),Y(10),TR(10),PR(10),CG(100,100)
      DATA CG(1,7),CG(1,8),CG(1,9),CG(2,7),CG(2,8),CG(2,9),
     1CG(3,7),CG(3,8),CG(3,9),CG(4,7),CG(4,8),CG(4,9),
     2CG(5,7),CG(5,8),CG(5,9),CG(6,7),CG(6,8),CG(6,9),
     3CG(7,8),CG(7,9),CG(8,9)/.036,.1,.085,.05,.13,.084,
     4.08,.135,.075,.09,.13,.06,.095,.13,.05,.095,.125,.065,
     5-.02,.18,.1/
      R=82.056
      ID=-1
      DO 97 I=1,NCOMP
      DO 97      J=1,NCOMP
      CG(J,I)=CG(I,J)
      A(I,J)=.0
      AM=.0
      BM=.0
      B(I)=.0
      AK(I)=.0
97    CONTINUE
10    FORMAT(10G)
      DO 1 I=1,NCOMP
      TR(I)=T/TC(I)
      IF(Y(I).EQ..0) GO TO 149
      PR(I)=P/PC(I)
      A(I,I)=.45724*(R*TC(I))**2/PC(I)
      B(I)=.0778*R*TC(I)/PC(I)
103   FORMAT(1X,'I,A(II)',I2,X,F15.3)
      AK(I)=.37464+1.54226*W(I)-.26992*W(I)**2
102   FORMAT(1X,'I,K',I2,X,F10.5)
      AK(I)=(1.+AK(I)*(1.-SQRT(TR(I))))**2
      A(1,I)=AK(I)*A(I,I)
30    FORMAT(1X,'TR,PR,A(I,I),B',5F13.4,X)
149   CONTINUE
1     CONTINUE
      DO 2 I=1,NCOMP
      DO 2 J=1,NCOMP
      IF(Y(J).EQ..0) GO TO 145
      IF(Y(I).EQ..0) GO TO 145
      A(I,J)=(1.-CG(I,J))*SQRT(A(I,I)*A(J,J))
81    FORMAT(1X,2(I2,X),F15.5)
145   CONTINUE
2     CONTINUE
      DO 4 I=1,NCOMP
      IF(Y(I).LE..0) GO TO 41
41    CONTINUE
      BM=BM+B(I)*Y(I)
4     CONTINUE
      DO 75      I=1,NCOMP
      AK(I)=.0
75    CONTINUE
```

```
        DO 3 J=1,NCOMP
        DO 3 I=1,NCOMP
        IF(Y(I).EQ..0) GO TO 148
        IF(Y(J).EQ..0) GO TO 148
        AK(J)=Y(I)*A(I,J)+AK(J)
148     CONTINUE
3       CONTINUE
        DO 6 J=1,NCOMP
        AK(J)=2.*AK(J)
85      FORMAT(1X,F15.4)
6       CONTINUE
  DO 5 I=1,NCOMP
  DO 5 J=1,NCOMP
        AM=AM+Y(I)*Y(J)*A(I,J)
5       CONTINUE
        CALL VCUBE(AM,BM,P,R,T,V,Z,ID)
        AB=AM*P/(R*T)**2
        BB=BM*P/(R*T)
        DO 62      I=1,NCOMP
        IF(Y(I).EQ..0) GO TO 61
        A1=B(I)*(Z-1.)/BM
        A2=ALOG(Z-BB)
        A3=AB/(2*SQRT(2.)*BB)
86      FORMAT(1X,4(F15.3,X))
        A4=AK(I)/AM-B(I)/BM
        A5=ALOG((Z+2.414*BB)/(Z-.414*BB))
84      FORMAT(1X,4(F10.4,X))
        PHI(I)=A1-A2-A3*A4*A5
        PHI(I)=EXP(PHI(I))
        PHI(I)=PHI(I)*Y(I)*P
61      CONTINUE
62      CONTINUE.
        RETURN
        END
```

```
            SUBROUTINE VCUBE(A,B,P,R,T,V,Z,ID)
            D=B-R*T/P
            E=-(3.*B*B+2.*R*T*B/P-A/P)
            F=B*B*B+(R*T*B*B-A*B)/P
              G=(3.*E-D*D)/3.
              H=-(9.*D*E-27.*F-2.*D*D*D)/27.
              IF(G**3./27.+H*H/4..LE.0.) GO TO 10
              S=-H/2.+SQRT(G**3./27.+H*H/4.)
              TT=-H/2.-SQRT(G**3./27.+H*H/4.)
              IF(S)5,6,6
      5         S=-((-S)**(1./3.))
              GO TO 7
      6       S=(S)**(1./3.)
      7       IF(TT)8,9,9
      8       TT=-(-TT)**(1./3.)
              GO TO 15
      9       TT=(TT)**(1./3.)
      C     SINGLE REAL ROOT
      15      V=S+TT-D/3.
              GO TO 40
      10      THETA = (ACOS(-.5*H/SQRT(-G**3/27.)))/3.
              V1=2.*SQRT(-G/3.)*COS(THETA)
              V2=2.*SQRT(-G/3.)*COS(THETA+2.0944)
              V3=2.*SQRT(-G/3.)*COS(THETA+4.1888)
              IF(ID)20,30,30
      C     TAKE LARGEST V FOR VAPOR
      20      V=AMAX1(V1,V2,V3)-D/3.
              GO TO 40
      C     TAKE SMALLEST V FOR LIQUID
      30    V=AMIN1(V1,V2,V3)-D/3.
      40    Z=P*V/(R*T)
            RETURN
            END
```

```
      SUBROUTINE ACT(SO1,SO2,SO3,SO4,T,ACTI,NCOMP,Y)
      DIMENSION SO1(10),SO2(10),SO3(10),SO4(10),X(10)
      DIMENSION Y(10)
      DO 1 I=1,NCOMP
      IF(I.EQ.6) GO TO 2
      X(I)=SO1(I)+SO2(I)/T+SO3(I)*ALOG(T)+SO4(I)*T
      X(I)=EXP(X(I)/1.987)
      IF(Y(I).EQ.0.0)X(I)=0.0
      XSUM=XSUM+X(I)
2     XX=.0
1     CONTINUE
8     FORMAT(1X,F10.8)
      XW=1.-XSUM
      ACTI=1.987*T*ALOG(XW)
      XSUM=.0
      IF(T.LT.273.16) ACTI=.0
      RETURN
      END
```